arXiv:hep-ph/0610091v1 9 Oct 2006

Strange meson-nucleon states in the quark potential model

Hai-Jun Wang and Jun-Chen Su
Center for Theoretical Physics, School of Physics, Jilin University, Changchun 130023, China

The quark potential model and resonating group method are used to investigate the $\overline{K}N$ bound states and/or resonances. The model potential consists of the t-channel and s-channel one-gluon exchange potentials and the confining potential with incorporating the QCD renormalization correction and the spin-orbital suppression effect in it. It was shown in our previous work that by considering the color octet contribution, use of this model to investigate the KN low energy elastic scattering leads to the results which are in pretty good agreement with the experimental data. In this paper, the same model and method are employed to calculate the masses of the $\overline{K}N$ bound systems. For this purpose, the resonating group equation is transformed into a standard Schrödinger equation in which a nonlocal effective $\overline{K}N$ interaction potential is included. Solving the Schrödinger equation by the variational method, we are able to reproduce the masses of some currently concerned $\overline{K}N$ states and get a view that these states possibly exist as $\overline{K}N$ molecular states. For the KN system, the same calculation gives no support to the existence of the resonance $\Theta^+(1540)$ which was announced recently.

I. INTRODUCTION

Recently, the $\overline{K}\,N$ systems has attracted much interest in investigations of the puzzle of exotic baryon state $\Lambda(1405)$ [1-9]. The puzzle of $\Lambda(1405)$ came from the obvious discrepancy between the downward shift of the $1S$ level of the kaonic hydrogen atom which was determined from the measurement of atomic x rays [10-12] and the upward shift measured from low energy $\overline{K}N$ scattering [13]. Although the discrepancy itself has been resolved recently by the elaborate measurement of x rays from the atom with an upward shift of the $1S$ level [14,15], how to understand the nature of the state has not reached its last word yet. The state seems to be able to be interpreted as an elementary baryon, i.e., a three quark state belongs to the 70^- multiplet, a meson-baryon composite being a $\overline{K}N$ bound state or a $\pi\Sigma$ resonance, or a five quark bound state. In Ref. [16], the authors investigated the state $\Lambda(1405)$ by employing a coupled-channel potential model with introducing a separable Yukawa-type meson-baryon potential. From fitting to low-energy $\overline{K}N$ scattering data, they obtained two sets of parameters: one allows them to interpret the state $\Lambda(1405)$ as the 70^- three-quark state strongly coupled with $\overline{K}N$ and $\pi\Sigma$; another to interpret the state as a $\pi\Sigma$ resonance and/or an unstable $\overline{K}N$ bound state. In Ref. [17], the s-wave meson-baryon interaction in the strangeness $S=-1$ sector was studied by means of a coupled channel method by using the lowest chiral Lagrangian. By a good fit to the scattering data, the authors conclude that the $\Lambda(1405)$ and $\Lambda(1670)$ may be identified with $\overline{K}N$ and $K\Xi$ quasibound states, respectively. The resonances $\Lambda(1405)$ and $\Lambda(1670)$ were also investigated in Ref. [18] in the Bethe-Salpeter coupled-channel formalism by utilizing the interaction given by the lowest perturbative chiral Lagrangian. In addition, the resonances $\Lambda(1405)$ and $\Sigma(1620)$ were ever studied in the QCD sum rule approach by using multiquark interpolating fields $((q\overline{q})(qqq))$ [19]. In this study, the above resonances are considered as multiquark states. In Ref. [20], the two-pole structure of $\Lambda(1405)$ was studied from the reaction $K^-p\to\pi^0\pi^0\Sigma^0$ in the energy region of $p_{K^-}=514$ to $750\ MeV/c$ by using the chiral unitary theory. The possible existence of deeply bound kaonic states was recently investigated for few-body systems by assuming a kaon-nucleon interaction of Gaussian type with a fixed width [21]. In this investigation, it was concluded that the $\Lambda(1405)$ may be viewed as a $\overline{K}N$ bound state. However, a critical analysis given in Ref. [22] on the KEK and FINUDA experiments [23] indicates that the experimental confirmation of the existence of deeply bound kaonic states is still under debate.

In our previous work [24], we have elaborately calculated the KN and $\overline{K}N$ elastic scattering phase shifts. The results are in quite good agreement with the experimental data and show that for the $\overline{K}N$ system, the s-wave shifts exhibit strong attractive interactions in the s-channel scattering, while, for the KN system, only the P_{01} and D_{03} states have small positive phase shifts which imply that the attractive interactions in these states are weak. The aim of this paper is to investigate the $\overline{K}N$ bound states and resonances by using the quark potential model and resonating group method (RGM) [25], and to discuss whether the pentaquark $\Theta^+(1540)$ [26-29] is possible to exist or not. The potential used is composed of the t-channel one gluon exchange potential (OGEP) [30] and the $s-$channel OGEP [24, 31-33] as well as a phenomenological confining potential. The two OGEPs were derived from QCD in the nonrelativistic approximation of order p^2/m^2 and contain spin-independent terms such as the Coulomb, velocity-dependent terms and spin-dependent terms such as the spin-spin interaction, spin-orbital coupling and tensor force terms. All these terms are taken into account in our investigation as should be done in a theoretically consistent

treatment. Especially, the s-channel OGEP is necessary to be considered for the $\overline{K}N$ interaction. With this potential and considering the contribution of color octet of clusters $K(\overline{K})$ and N, it was demonstrated in our previous works [24, 32, 33] that the model is not only able to quite well reproduce the KN low-energy elastic scattering data, but also to give reasonable results for the $\pi\pi$ low-energy scattering and $K\overline{K}$ bound states. The results obtained in our previous works encourage us to study $\overline{K}N$ and KN resonances $\Lambda(1405)$, $\Lambda(1600)$, $\Lambda(1670)$, $\Sigma(1385)$, $\Sigma(1620)$ and $\Theta^+(1540)$ in a consistent way within the framework of the aforementioned potential model and RGM.

II. FORMALISM

In this section, we briefly describe the potential model and resonating group method (RGM). According to the quark model, the KN ($\overline{K}N$) system may be treated as two quark clusters: the K-cluster ($q\overline{s}$) (the $\overline{K}$-cluster ($\overline{q}s$)) and the N-cluster (qqq) where $q = u$ or d. The effective KN ($\overline{K}N$) interaction potential may be extracted from the following Schrödinger equation for the interacting $q^4\overline{s}$ ($q^3\overline{q}s$) system by the RGM [25]

$$(T + V)\Psi = E\Psi \tag{1}$$

where E, T, V and Ψ stand for the total energy, the kinetic energy, the interaction potential and the wave function of the multiquark system, respectively.

A. Interquark potential

In the center of mass frame, the kinetic energy is given by

$$T = \sum_{i=1}^{5} \frac{\vec{p}_i^2}{2m_i} - T_c \tag{2}$$

where T_c represents the center of mass kinetic energy, The interaction potential is assumed to be

$$V = \sum_{i<j=1}^{5} (V_{ij}^t + V_{ij}^s + V_{ij}^c) \tag{3}$$

where V_{ij}^t, V_{ij}^s and V_{ij}^c denote the t-channel OGEP, the s-channel OGEP and the confining potentials, respectively. They are separately described in the following.

The t-channel OGEP represented in the momentum space is [24, 30]

$$\begin{aligned} V_{ij}^t = {} & \frac{4\pi\alpha_s C_{ij}^t}{(\vec{q}-\vec{k})^2}\{1 - \frac{\vec{P}^2}{m_{ij}^2} - \frac{(m_i^2+m_j^2)}{8m_i^2m_j^2}(\vec{q}-\vec{k})^2 + \frac{(m_i-m_j)}{2m_im_jm_{ij}}\vec{P}\cdot(\vec{q}+\vec{k}) \\ & + \frac{(\vec{q}+\vec{k})^2}{4m_im_j} + \frac{i}{4m_{ij}}[\vec{P}\cdot(\vec{q}-\vec{k})\cdot(\frac{\vec{\sigma}_i}{mi} - \frac{\vec{\sigma}_j}{m_j})] - \frac{(\vec{q}-\vec{k})^2}{4m_im_j}\vec{\sigma}_i\cdot\vec{\sigma}_j \\ & + \frac{i}{4m_{ij}}(\vec{q}\times\vec{k})\cdot[(2+\frac{m_j}{m_i})\vec{\sigma}_i + (2+\frac{m_i}{m_j})\vec{\sigma}_j] + \frac{(\vec{q}-\vec{k})\cdot\vec{\sigma}_i(\vec{q}-\vec{k})\cdot\vec{\sigma}_j}{4m_im_j}\} \end{aligned} \tag{4}$$

where $m_{ij} = m_i + m_j$ with m_i and m_j being the masses of i-th and j-th quarks respectively, α_s is the QCD fine structure constant, $\vec{\sigma}_i$and $\vec{\sigma}_j$are the spin Pauli matrices for i-th and j-th quarks, C_{ij}^t is the t-channel color matrix defined as

$$C_{ij}^t = \begin{cases} \frac{\lambda_i^a}{2}\frac{\lambda_j^a}{2}(\frac{\lambda_i^{a*}}{2}\frac{\lambda_j^{a*}}{2}), & \text{for } qq(\overline{qq}) \\ -\frac{\lambda_i^a}{2}\frac{\lambda_j^{a^*}}{2}, & \text{for } q\overline{q} \end{cases} \tag{5}$$

with λ^a being the Gell-Mann matrix, $\vec{P}, \vec{k}$ and $\vec{q}$ are respectively the total momentum, the initial state relative momentum and the final state relative momentum of the two interacting particles.

The s-channel OGEP is [24, 31-33]

$$\begin{aligned} V_{ij}^s = {} & \frac{\pi\alpha_s F_{ij}^s C_{ij}^s}{2mm'}[(3 + \vec{\sigma}_i\cdot\vec{\sigma}_j) - \frac{5(m^2+m'^2)-4mm'}{8m^2m'^2}\vec{P}^2 - \frac{2\vec{k}^2}{m^2} - \frac{2\vec{q}^2}{m'^2} \\ & - (\frac{(m^2+m'^2)}{8m^2m'^2} + \frac{\vec{k}^2}{m^2} + \frac{\vec{q}^2}{m'^2})\vec{\sigma}_i\cdot\vec{\sigma}_j + \frac{i}{4m'^2}(\vec{P}\times\vec{q})\cdot(\vec{\sigma}_i - \vec{\sigma}_j) \\ & - \frac{i}{4m^2}(\vec{P}\times\vec{k})\cdot(\vec{\sigma}_i - \vec{\sigma}_j) - \frac{(m-m')^2}{4m^2}\vec{P}\cdot\vec{\sigma}_i\vec{P}\cdot\vec{\sigma}_j \\ & + \frac{1}{4m^2}(\vec{P}\cdot\vec{\sigma}_i\vec{k}\cdot\vec{\sigma}_j - \vec{k}\cdot\vec{\sigma}_i\vec{P}\cdot\vec{\sigma}_j + 4\vec{k}\cdot\vec{\sigma}_i\vec{k}\cdot\vec{\sigma}_j) \\ & + \frac{1}{4m'^2}(\vec{P}\cdot\vec{\sigma}_i\vec{q}\cdot\vec{\sigma}_j - \vec{q}\cdot\vec{\sigma}_i\vec{P}\cdot\vec{\sigma}_j + 4\vec{q}\cdot\vec{\sigma}_i\vec{q}\cdot\vec{\sigma}_j)] \end{aligned} \tag{6}$$

where m and m' denote the quark (antiquark) masses before and after annihilation respectively, C_{ij}^s and F_{ij}^s are respectively the s-channel color and flavor matrices defined by

$$C_{ij}^s = \frac{1}{24}(\lambda_i^a - \lambda_j^{a^*})^2 \tag{7}$$

here λ_i^a are the Gell-Mann matrices for i-th quark and

$$F_{ij}^s = \frac{1}{3} - (\frac{1}{2}\vec{\tau}_i \cdot \vec{\tau}_j + V_i^- V_j^+ + V_i^+ V_j^- + U_i^- U_j^+ + U_i^+ U_j^- + \frac{3}{2} Y_i Y_j) \tag{8}$$

here $\vec{\tau_i}$ are the isospin Pauli matrices for i-th particle, Y_i the hypercharge operators, V_i^+ and V_i^- (U_i^+ and U_i^-) represent the rising and lowering operators of the V-spin (U-spin) respectively. The s-channel OGEP gives nonvanishing S-matrix elements only for $\overline{K}N$ system

The confining potential, as was done in Ref. [32], is taken to be a harmonic oscillator one. In momentum space, it is represented as

$$V_{ij}^c = C_{ij}^t (2\pi)^3 \mu_{ij} \omega^2 \nabla_k^2 \delta^3(\vec{q} - \vec{k}) \tag{9}$$

where μ_{ij} is the reduced mass of two interacting particles and ω the force-strength parameter.

B. Resonating group method

In application of resonating group method to investigate the system of composite particles, we need to give the basis wave function of the system. Let us first construct the basis function of KN system from the wave functions of clusters $(q\overline{s})$ and (qqq). Since there are identical particles between the two clusters, the basis function of the system may be represented as

$$\begin{aligned} &\Phi_{TM\frac{1}{2}m}(\vec{p}_1, \vec{p}_2, \vec{p}_3, \vec{p}_4, \vec{p}_5; \vec{\rho}) \\ &= \mathcal{A}\Psi_{TM\frac{1}{2}m}(1,2,3,4,5) R(\vec{p}_1, \vec{p}_2, \vec{p}_3, \vec{p}_4, \vec{p}_5; \vec{\rho}) \end{aligned} \tag{10}$$

where the three quarks in the N-cluster are labeled as $1, 2, 3$ and the quark and antiquark in the K-cluster (or the antiquark and quark in the $\overline{K}$-cluster) as 4 and 5, $\Psi_{TM\frac{1}{2}m}(1,2,3,4,5)$ and $R(\vec{p}_1, \vec{p}_2, \vec{p}_3, \vec{p}_4, \vec{p}_5; \vec{\rho})$ represent the color-isospin-spin wave function and the position space wave function respectively which are constructed from the color-isospin-spin wave functions and the coordinate space wave functions of nucleon and kaon,

$$\mathcal{A} = \frac{1}{\sqrt{4}}(1 - P_{14} - P_{24} - P_{34}) \tag{11}$$

denotes the antisymmetrized operator in which P_{j4} $(j = 1, 2, 3)$ symbolize the interchange operators. For the $\overline{K}N$ system, noticing that there is no identical particles between the two clusters $(\overline{q}s)$ and (qqq), the basis wave function of the system may simply be written out from Eq. (10) by setting $\mathcal{A} = 1$. In this case, $\Psi_{TM\frac{1}{2}m}(1,2,3,4,5)$ and $R(\vec{p}_1, \vec{p}_2, \vec{p}_3, \vec{p}_4, \vec{p}_5; \vec{\rho})$ are the color-isospin-spin wave function and the position space wave function constructed from the corresponding wave functions of nucleon and antikaon.

When kaon (antikaon) and nucleon interact, the color states of the two quark clusters are possibly polarized. In this case, the kaon (antikaon) and nucleon should not be viewed as pure color singlet objects even though the whole system is kept in color singlet and therefore the interaction taking place in the color octet must be taken into account. Consideration of color octet channel interactions has been proved to be important to reproduce experimental data in the investigations of hadron productions and decays [34-36]. Thus, the color-spin-isospin wave function $\Psi_{TM\frac{1}{2}m}(1,2,3,4,5)$ of the whole system may be given by the color singlet part $\Psi^{(1)}_{TM\frac{1}{2}m}(1,2,3,4,5)$ or the color octet part $\Psi^{(2)}_{TM\frac{1}{2}m}(1,2,3,4,5)$ formed by the color singlets or color octets of the two clusters. In principle, we may test a general color structure of system under consideration which is given by the following linear combination

$$\Psi_{TM\frac{1}{2}m}(1,2,3,4,5) = \alpha\Psi^{(1)}_{TM\frac{1}{2}m}(1,2,3,4,5) + \beta\Psi^{(2)}_{TM\frac{1}{2}m}(1,2,3,4,5) \tag{12}$$

where the coefficients α and β are required to satisfy

$$|\alpha|^2 + |\beta|^2 = 1. \tag{13}$$

The wave functions $\Psi^{(1)}_{TM\frac{1}{2}m}(1,2,3,4,5)$ and $\Psi^{(2)}_{TM\frac{1}{2}m}(1,2,3,4,5)$, as described in Appendix A, were constructed in Ref. [24] by the antisymmetric requirement for the wave functions of identical particles in nucleon.

Because we limit our discussion to the interaction in the low-energy regime, it is appropriate to write the position space basis function of the KN or $\overline{K}N$ system in the form

$$R(\vec{p}_1,\vec{p}_2,\vec{p}_3,\vec{p}_4,\vec{p}_5;\vec{\rho}) = \phi^{(+)}_{os}(\vec{p}_1,\vec{\rho})\phi^{(+)}_{os}(\vec{p}_2,\vec{\rho})\phi^{(+)}_{os}(\vec{p}_3,\vec{\rho})\phi^{(-)}_{os}(\vec{p}_4,\vec{\rho})\phi^{(-)}_{os}(\vec{p}_5,\vec{\rho}) \tag{14}$$

where $\phi^{(+)}_{os}(\vec{p}_i,\vec{\rho})$ and $\phi^{(-)}_{os}(\vec{p}_j,\vec{\rho})$ are the lowest-lying harmonic oscillator states of the N-cluster and $K(\overline{K})$-cluster given in the momentum space,

$$\phi^{(\pm)}_{os}(\vec{p}_i,\vec{\rho}) = (2\sqrt{\pi}b_i)^{3/2}\exp(-\frac{1}{2}b_i^2\vec{p}_i^2 \mp i\lambda_\pm \vec{p}_i\cdot\vec{\rho}) \tag{15}$$

in which $\vec{\rho}$ is the vector representing the separation between the centers of mass of the two clusters and parameters $\lambda_\pm$ are defined by

$$\lambda_- = \beta_1 = \frac{3m_1}{4m_1+m_2}, \lambda_+ = \beta_2 = \frac{m_1+m_2}{4m_1+m_2} \tag{16}$$

here m_1 denotes the mass of d or u quark, m_2 the mass of strange quark. The wave function in Eq. (14) can be represented through the cluster coordinates in the form

$$R(\vec{p}_1,\vec{p}_2,\vec{p}_3,\vec{p}_4,\vec{p}_5;\vec{\rho}) = X_K(\vec{q})X_N(\vec{k}_1,\vec{k}_2)\Gamma(\vec{Q},\vec{\rho})Z_{CM}(\vec{P}) \tag{17}$$

where $X_K(\vec{q})$ and $X_N(\vec{k}_1,\vec{k}_2)$ are the internal motion wave functions of the $K(\overline{K})$-cluster $(q\overline{s})$ $((\overline{q}s))$ and the N-cluster (qqq) with $\vec{q}$ and $\vec{k}_1,\vec{k}_2$ being the relative momenta in the clusters $(q\overline{s})$ $((\overline{q}s))$ and (qqq) respectively, $\Gamma(\vec{Q},\vec{\rho})$ is the wave function describing the relative motion between the two clusters with $\vec{Q}$ being the relative momentum of the two clusters and $Z_{CM}(\vec{P})$ the wave function for the center-of-mass motion of the whole system in which $\vec{P}$ is the total momentum of the system. According to the RGM, the wave function of the two clusters may be represented in the form

$$\overline{\Psi}_{TMsm} = \int d^3\rho \Phi_{TM\frac{1}{2}m_s}(\vec{p}_1,\vec{p}_2,\vec{p}_3,\vec{p}_4,\vec{p}_5;\vec{\rho})f(\vec{\rho}) \tag{18}$$

where $\Phi_{TM\frac{1}{2}m_s}(\vec{p}_1,\vec{p}_2,\vec{p}_3,\vec{p}_4,\vec{p}_5;\vec{\rho})$ is the basis function defined in Eq. (10) and $f(\vec{\rho})$ is the unknown function describing the relative motion of the two clusters. On substituting the above wave function in Eq. (1), according to the well-known procedure, one may derive a resonating group equation satisfied by the function $f(\vec{\rho})$ which is obtained from Eq. (1) by subtracting the internal motion of the two clusters,

$$\int d^3\rho[T_r(\vec{\rho},\vec{\rho}') + V_r(\vec{\rho},\vec{\rho}') - E_r N_r(\vec{\rho},\vec{\rho}')]f(\vec{\rho}') = 0 \tag{19}$$

where

$$X(\vec{\rho},\vec{\rho}') = \int\prod_{i=1}^{5}\frac{d^3p_k}{(2\pi)^3}\frac{d^3p'_k}{(2\pi)^3}\langle\Phi_{TM\frac{1}{2}m}(\vec{p}_1,\vec{p}_2,\vec{p}_3,\vec{p}_4,\vec{p}_5;\vec{\rho}) \mid \mathcal{A}X \mid \Phi_{TM\frac{1}{2}m}(\vec{p}_1,\vec{p}_2,\vec{p}_3,\vec{p}_4,\vec{p}_5;\vec{\rho}')\rangle \tag{20}$$

here X stands for T, V or I (the unity). The expressions of the functions $T_r(\vec{\rho},\vec{\rho}')$, $V_r(\vec{\rho},\vec{\rho}')$ and $N_r(\vec{\rho},\vec{\rho}')$ are not shown here but will be used to derive the effective potential as described soon later.

C. Schrödinger equation and effective $KN(\overline{K}N)$ potential

The resonating group equation in Eq. (19) is not of the standard form of Schrödinger equation since the normalization function $N_r(\vec{\rho},\vec{\rho}')$ is not unity. It can be converted into a Schrödinger equation by the following transformation

$$f(\vec{\rho}) = \int d^3R\Gamma(\vec{\rho},\vec{R})\overline{\Psi}(\vec{R}) \tag{21}$$

where

$$\Gamma(\vec{\rho}.\vec{R}) = \frac{1}{\sqrt{2}(2\pi)^3}(\frac{3\beta_2}{\pi b^2})^{3/4}\int d^3k e^{\frac{1}{6\beta_2}b^2\vec{k}^2+i\vec{k}\cdot(\vec{\rho}-\vec{R})} \tag{22}$$

in which b is the harmonic oscillator size parameter and $\overline{\Psi}(\vec{R})$ will be identified with the wave function describing the relative motion of the two clusters. On inserting Eq. (21) into Eq. (19), it is not difficult to get

$$-\frac{1}{2\mu}\nabla^2_{\vec{R}}\overline{\Psi}(\vec{R}) + \int d^3R^{'}V(\vec{R},\vec{R}')\overline{\Psi}(\vec{R}') = \varepsilon\overline{\Psi}(\vec{R}) \tag{23}$$

where ε stands for the binding energy, μ denotes the reduced mass of nucleon and kaon (antikaon) and

$$V(\vec{R},\vec{R}') = V^t(\vec{R},\vec{R}') + V^s(\vec{R},\vec{R}') + V^c(\vec{R},\vec{R}') \tag{24}$$

is the nonlocal KN ($\overline{K}N$) effective interaction potential in which $V^t(\vec{R},\vec{R}')$, $V^s(\vec{R},\vec{R}')$ and $V^c(\vec{R},\vec{R}')$ are generated by the t-channel OGEP, the s-channel OGEP and the confining potential respectively. The potential $V(\vec{R},\vec{R}')$ in the Schrödinger equation is connected with the potential $V(\vec{\rho},\vec{\rho}')$ appearing in the resonating group equation by the following formula.

$$V(\vec{R},\vec{R}') = \int d^3\rho d^3\rho^{'}\Gamma(\vec{R},\vec{\rho})V(\vec{\rho},\vec{\rho}')\Gamma(\vec{\rho}',\vec{R}'). \tag{25}$$

Through a lengthy derivation, we obtain an explicit expression of the potential $V(\vec{R},\vec{R}')$ which is displayed in Appendix B.

III. NUMERICAL RESULTS

As mentioned before, use of the above effective potential to calculate the KN elastic scattering phase shifts leads to the results which are in reasonable agreement with experimental data. In this paper, we recalculate the phase shifts and find that a quite good fit to the experimental data can also be achieved by appropriately increasing both the coupling constant and the size parameter of harmonic oscillator with remaining other parameters unchanged. Some phase shifts selected here are shown in Figs.1-4 in which Figs. 1 and 2 give the theoretical prediction for some $\overline{K}N$ low energy elastic scattering phase shifts. These phase shifts are all positive, implying that the interactions in the relevant states are attractive and therefore possibly form bound states or resonances in those states. It is noted that in our present investigation, besides the color octet mechanism, the QCD renormalization effect and the spin-orbital suppression are also taken into account. In the calculations, the theoretical parameters are taken to be: the coupling constant $\alpha_s^0 = 0.527$, the force strength of confinement $\omega = 0.2\ GeV$, the harmonic oscillator size parameter $b = 0.483$, the constituent quark masses $m_u = m_d = 350MeV$ and $m_s = 550\ MeV$, the color combination coefficient $\alpha = 0.915$, the scale parameter of QCD renormalization $\mu = 0.195\ GeV$ and the parameter of spin-orbital suppression $\gamma = 0.45$. Except for the parameter α, all the parameters are consistently used in calculations of $S = -1$ $\overline{K}N$ states and $S = +1$ KN states.

The mass spectrum of $\overline{K}N$ bound and resonant states are calculated from the Schrödinger equation written in Eq. (23) by the variational method. The trial wave functions are chosen to be

$$\Psi(J,T) = \frac{1}{\sqrt{2J+1}}\sum_{nLS}\sum_{m_l m} u(n,L,S,)C^{Jm_J}_{Lm_lSm}R_{nLm_l}\Psi_{TSm} \tag{26}$$

where R_{nLm_l} stands for the coordinate space basis functions which are, as usual, taken to be the harmonic oscillator wave functions, Ψ_{TSm} represents the spin-isospin wave function of the two clusters with $S = 1/2$, and $u(n,L,S)$ are the unknown combination coefficients which can be determined by solving the Schrödinger equation. Here the quantum numbers of a state is represented by the conventional notation $L_{T\ 2J}(J^P)$ where L, J,T and P designate the orbital angular momentum, the total angular momentum, the isospin and parity of the state. It should be noted that the spin-isospin wave function Ψ_{TSm} in Eq. (26) is written formally. In the practical calculation, the effective potential in Eq. (23) is given by the matrix element of the potential operator shown in Appendix B between the color-spin-isospin wave function represented in Eq. (12) and Appendix A. In this kind of calculation, the wave function Ψ_{TSm} in Eq. (26) is replaced by the color-spin-isospin wave function mentioned above. Another point we would like to note is that

in solving the Schrödinger equation, the series over n in Eq. (26) is cut off by a limitation of $N = 2n + L$. We found that to obtain sufficiently accurate results, the N is unnecessarily taken to be large. To solve the binding energy from the Schrödinger equation, we choose the dimensionless parameter $a = \sqrt{m\omega}$ as the variational parameter which is determined by the following stationary condition

$$\frac{\partial \varepsilon}{\partial a} = 0. \tag{27}$$

The mass of a $\overline{K}$ $(K)N$ bound state or resonance is given by

$$M = m_1 + m_2 + \varepsilon \tag{28}$$

where m_1 and m_2 are the masses of constituent $K(\overline{K})$ and N clusters.

In this paper, we first limit ourself to focus our attention on the $\overline{K}N$ states $\Lambda(1405)$, $\Lambda(1600)$, $\Lambda(1670)$, $\Sigma(1385)$ and $\Sigma(1620)$ which were discussed in the previous literature. Within the prescription of RGM, these states are naturally treated as $\overline{K}N$ molecules with negative strangeness. The calculated masses of these states as well as the experimental ones are listed in Table 1. In our calculation, except for the color parameter α, the other parameters are taken to be the same as used in the scattering case. The color parameter which represents the color polarization describes the color structure of a state which characterizes, to some extent, the internal quark-gluon structure of the state. Obviously, the parameter α in bound states would be different from that in scattering processes. For the low energy elastic scattering, in general, only peripheral interactions are concerned. Apparently, in this case, the kaon (antikaon) and nucleon suffer from a slight color polarization in the interacting region and in the initial state and final state, they are, as free particles, still in color singlets. In our test, we find, when we take the combination parameter $\alpha = 0.915$, which means that the color singlet interaction between kaon (antikaon) and nucleon dominates, the scattering data may be fairly reproduced. However, in bound states and resonances, the kaon (antikaon) and nucleon are bounded together and even overlapped. In this case, a strong color polarization would happen. That is to say, the kaon (antikaon) and nucleon in the bound states and resonances, in general, can not exist as color singlet objects. Since the color structure or the quark-gluon structures for different bound states and resonances are different, the effective interactions taking place in those states would be different from one another. According to our calculation, the $\Lambda(1405)$ is identified with a lowest $\overline{K}N$ bound state with the quantum numbers $S_{0\ 1}(\frac{1}{2}^-)$ and color parameter $\alpha = 0.91$ which implies that the both clusters $\overline{K}(\overline{q}s)$ and $N(q^3)$ in the s-shell state are almost kept in their color singlets. While, the $\Lambda(1600)$, $\Lambda(1670)$, $\Sigma(1385)$ and $\Sigma(1620)$ are excited molecular states with quantum numbers $P_{0\ 1}(\frac{1}{2}^+)^*$, $S_{0\ 1}(\frac{1}{2}^-)^*$, $P_{1\ 3}(\frac{3}{2}^+)^*$ and $S_{1\ 1}(\frac{1}{2}^-)^*$, respectively. The state $\Lambda(1600)$ is a p-shell resonance and the $\Lambda(1670)$ is a first radial-excited s-shell resonance both of which are isoscalar states. While, $\Sigma(1385)$ and $\Sigma(1620)$ are the isovectorial p-shell and s-shell states. The smaller values of the parameter α for these states indicate that they have rather complicated quark-gluon structures. Particularly, for the resonance state $\Sigma(1385)$, since the α is too small, there is a small amount of singlet-singlet component in this state and, therefore, it cannot be viewed as an ordinary meson-baryon molecule. Such a state looks like an exotic baryon state containing four valence quarks and one valence antiquarks. As we learn from particle physics, colored quark and/or antiquark pairs and gluons as well as their colored clusters existing in the intermediate state of a process or in the interaction region of an hadron system will decay into various color singlet hadrons in the final state. Therefore, working in the hadron dynamics, to investigate the problems of decay, scattering and bound states for hadron systems, it is natural to introduce various meson exchange potentials and to perform coupled channel calculations where all hadrons involved are treated from beginning to end as color singlet objects. Nevertheless, when we work in the quark potential model and introduce the color octet mechanism, consideration of the meson exchanges may be unnecessary.

States	$\Lambda(1405)$	$\Lambda(1600)$	$\Lambda(1670)$	$\Sigma(1385)$	$\Sigma(1620)$
$L_{I\ 2J}(J^P)$	$S_{0\ 1}(\frac{1}{2}^-)$	$P_{0\ 1}(\frac{1}{2}^+)^*$	$S_{0\ 1}(\frac{1}{2}^-)^*$	$P_{1\ 3}(\frac{3}{2}^+)^*$	$S_{1\ 1}(\frac{1}{2}^-)^*$
α	0.91	0.83	0.723	0.21	0.81
Theor. masses (MeV)	1405	1603	1667	1384	1617
Expt. masses (MeV)	1405±10	1596±6	1670±5	1385±3	1633±10

TABLE I. Masses of exotic states S=-1

Now let us turn to the resonance $\Theta^+(1540)$. Whether this state exists or not nowadays is still in debate. Some experiments supported its existence, but some other experiments failed to find it [28]. In this paper, we have calculated the KN states by the same procedure as for the $\overline{K}N$ states, trying to find if a resonance could be formed in the P_{01} state or the D_{03} state. In the calculation, we use the parameters as determined in the study of KN scattering except that the parameter α is chosen to be a adjustable parameter. But, in our test, we find, even though in these two states, as mentioned before, the interactions are attractive, it is impossible to find an appropriate α which could give a state with the mass $1540MeV$ and $IJ^P = 0\frac{1}{2}^+$ [37] or $IJ^P = 0\frac{3}{2}^-$[38, 39]. The reason is probably due to that the attractive interactions in those states are too weak for forming a bound state or a resonance.

IV. SUMMARY

In this paper, the states $\Lambda(1405)$, $\Lambda(1600)$, $\Lambda(1670)$, $\Sigma(1385)$, $\Sigma(1620)$ and $\Theta^+(1540)$ were investigated in the constituent quark potential model within the framework of RGM. The distinctive feature of the investigation is that the effective interaction potential between the strange meson and nucleon was merely derived from QCD-inspired interquark potential with incorporating the QCD renormalization correction and the spin-orbital suppression effect in it without concerning any meson exchanges. With considering the contribution arising from the color octets of the clusters $\overline{K}(\overline{q}s)$ (or $K(q\overline{s})$) and $N(q^3)$, the potential model used is able to reasonably reproduce the KN low energy scattering data and gives some prediction of the $\overline{K}N$ low energy elastic scattering phase shifts. With the theoretical parameters are determined by fitting the scattering data, the model calculation allows us to interpret the states $\Lambda(1405)$, $\Lambda(1600)$, $\Lambda(1670)$, $\Sigma(1385)$ and $\Sigma(1620)$ as $\overline{K}N$ molecular states with a certain color structures characterized by the parameter α and gives no support to the existence of the pentaquark state $\Theta^+(1540)$. Certainly, the validity of the model used in this paper needs to be verified by further investigations on other hadron systems and on the problem of resonance decays. In particular, to confirm the color structures of the $\overline{K}N$ molecular states, it is expected that more accurate lattice QCD calculations of the states would appear in the future. Moreover, to justify the results given in our calculation, experimental $\overline{K}N$ elastic scattering phase shifts given in the low energy domain are urgently anticipated.

V. ACKNOWLEDGMENT

This project was supported in part by the National Natural Science Foundation of China and Youth Foundation of Jilin University.

VI. APPENDIX A: THE COLOR-FLAVOR-SPIN WAVE FUNCTIONS

In general, the color singlet color state of the five quark cluster $(q^4\overline{s})$ or $(q^3\overline{q}s)$ may be built up by the color singlets of the N-cluster (qqq) and K-cluster $(q\overline{s})$ (or the $\overline{K}$-cluster $(\overline{q}s)$) or the color octets of the two subclusters. Correspondingly, for the five quark cluster, there are two classes of color-flavor-spin wave functions denoted by $\Psi^{(1)}_{TM\frac{1}{2}m}(1,2,3,4,5)$ and $\Psi^{(2)}_{TM\frac{1}{2}m}(1,2,3,4,5)$ which are color singlets as a whole, but associated respectively with the color singlets and the color octets of the two subclusters. In the function $\Psi^{(1)}_{TM\frac{1}{2}m}(1,2,3,4,5)$, the color-flavor-spin (CFS) wave function $\Psi^{(1)}_{\frac{1}{2}M_1\frac{1}{2}m_s}(1,2,3)_N$ for the N-cluster which is of the symmetry denoted by the Young diagram $[1^3]_{cfs}$ and hence totally antisymmetric) is constructed from the C-G coupling of $[1^3]_C \times [3]_{FS}$ where $[1^3]_C$ and $[3]_{FS}$ are the Young diagrams denoting the antisymmetric color singlet and the symmetric flavor-spin states respectively. In the function $\Psi^{(2)}_{TM\frac{1}{2}m}(1,2,3,4,5)$, the antisymmetric CFS wave function $\Psi^{(1)}_{\frac{1}{2}M_1\frac{1}{2}m_s}(1,2,3)_N$ for the N-cluster is given by the C-G coupling of $[21]_C \times [21]_{FS}$ where $[21]_C$ and $[21]_{FS}$ represent the color octet state and the flavor-spin state of mixed symmetry respectively. The explicit expressions of the wave functions mentioned above can easily be written out by the familiar method given in the group theory, as displayed in the following.

The first class of the CFS wave function in Eq. (12) for the whole system is

$$\Psi^{(1)}_{TM\frac{1}{2}m}(1,2,3,4,5) = \sum_{M_1M_2} C^{TM}_{\frac{1}{2}M_1\frac{1}{2}M_2}\Psi^{(1)}_{\frac{1}{2}M_1\frac{1}{2}m}(1,2,3)_N\Psi^{(1)}_{\frac{1}{2}M_200}(4,5)_K \tag{A1}$$

where $\Psi^{(1)}_{\frac{1}{2}M_1\frac{1}{2}m}(1,2,3)_N$, as mentioned before, is the CFS wave function for the N-cluster and $\Psi^{(1)}_{\frac{1}{2}M_200}(4,5)_K$ is the CFS wave function for the K-cluster. They are represented separately as

$$\Psi^{(1)}_{\frac{1}{2}M_1\frac{1}{2}m_s}(1,2,3)_N = \xi^0_c(1,2,3)\chi^{(1)}_{\frac{1}{2}M_1\frac{1}{2}m_s}(1,2,3) \tag{A2}$$

where

$$\xi^0_c(1,2,3) = \frac{1}{\sqrt{6}}\epsilon_{abc}q^a(1)q^b(2)q^c(3) \tag{A3}$$

represents the color singlet wave function of the N-cluster and

$$\chi^{(1)}_{\frac{1}{2}M_1\frac{1}{2}m_s}(1,2,3) = \frac{1}{\sqrt{2}}[\chi^a_{\frac{1}{2}M_1}(1,2,3)\varphi^a_{\frac{1}{2}m_s}(1,2,3) + \chi^b_{\frac{1}{2}M_1}(1,2,3)\varphi^b_{\frac{1}{2}m_s}(1,2,3)] \tag{A4}$$

is the isospin-spin wave function of the N-cluster in which the isospin wave functions $\chi^a_{\frac{1}{2}M_1}(1,2,3)$ and $\chi^b_{\frac{1}{2}M_1}(1,2,3)$ and the spin wave functions $\varphi^a_{\frac{1}{2}m_s}(1,2,3)$ and $\varphi^a_{\frac{1}{2}m_s}(1,2,3)$ are expressed as follows

$$\begin{aligned}
\chi^a_{\frac{1}{2}M_1}(1,2,3) &= \sum_{m,m_3,m_1,m_2} C^{\frac{1}{2}M_1}_{1m\frac{1}{2}m_3} C^{1m}_{\frac{1}{2}m_1\frac{1}{2}m_2}\chi_{\frac{1}{2}m_1}(1)\chi_{\frac{1}{2}m_2}(2)\chi_{\frac{1}{2}m_3}(3)\\
\chi^b_{\frac{1}{2}M_1}(1,2,3) &= \sum_{m_1,m_2,m_3} C^{\frac{1}{2}M_1}_{00\frac{1}{2}M_1} C^{00}_{\frac{1}{2}m_1\frac{1}{2}m_2}\chi_{\frac{1}{2}m_1}(1)\chi_{\frac{1}{2}m_2}(2)\chi_{\frac{1}{2}m_3}(3)\\
\varphi^a_{\frac{1}{2}m_s}(1,2,3) &= \sum_{m,m_3,m_1,m_2} C^{\frac{1}{2}m_s}_{1m\frac{1}{2}m_3} C^{1m}_{\frac{1}{2}m_1\frac{1}{2}m_2}\varphi_{\frac{1}{2}m_2}(1)\varphi_{\frac{1}{2}m_2}(2)\varphi_{\frac{1}{2}m_3}(3)\\
\varphi^b_{\frac{1}{2}m_s}(1,2,3) &= \sum_{m_1,m_2,m_3} C^{\frac{1}{2}m_s}_{00\frac{1}{2}m_s} C^{00}_{\frac{1}{2}m_1\frac{1}{2}m_2}\varphi_{\frac{1}{2}m_2}(1)\varphi_{\frac{1}{2}m_2}(2)\varphi_{\frac{1}{2}m_3}(3)
\end{aligned} \tag{A5}$$

The CFS wave function of the K- cluster is

$$\Psi^{(1)}_{\frac{1}{2}M00}(4,5)_K = C_0(4,5)\chi_{\frac{1}{2}M}(4,5)\varphi_{00}(4,5) \tag{A6}$$

where $C_0(4,5)$, $\chi_{\frac{1}{2}M}(4,5)$ and $\varphi_{00}(4,5)$ are the color, isospin and spin wave functions, respectively. Since there is no identical particles in the cluster, these wave functions are of the forms

$$C_0(4,5) = \frac{1}{\sqrt{3}}q^a(4)\overline{q}^a(5) \tag{A7}$$

and

$$\begin{aligned}
\chi_{\frac{1}{2}M}(4,5) &= \sum_{m_1\ m_2} C^{\frac{1}{2}M}_{\frac{1}{2}m_100}\chi_{\frac{1}{2}m_1}(4)\chi_{00}(5)\\
\varphi_{00}(4,5) &= \sum_{m_1\ m_2} C^{00}_{\frac{1}{2}m_1\frac{1}{2}m_2}\varphi_{\frac{1}{2}m_1}(4)\varphi_{\frac{1}{2}m_2}(5)
\end{aligned} \tag{A8}$$

For the second class of the CFS wave function in Eq. (12), it can be represented as

$$\Psi^{(2)}_{TM\frac{1}{2}m}(1,2,3,4,5) = \sum_{M_1M_2}\sum_c C^{TM_T}_{\frac{1}{2}M_1\frac{1}{2}M_2}\Psi^{(2)c}_{\frac{1}{2}M_1\frac{1}{2}m}(1,2,3)_N\Psi^{(2)c}_{\frac{1}{2}M00}(4,5)_K \tag{A9}$$

where $\Psi^{(2)c}_{\frac{1}{2}M_1\frac{1}{2}m}(1,2,3)_N$ and $\Psi^{(2)c}_{\frac{1}{2}M00}(4,5)_K$ are the second class of CFS wave functions for the N-cluster and the K-cluster respectively. Their expressions are shown in the following.

$$\Psi^{(2)C}_{\frac{1}{2}M_1\frac{1}{2}m_s}(1,2,3)_N = \frac{1}{\sqrt{2}}[\xi^A_c(1,2,3)\chi^{(2)B}_{\frac{1}{2}M_1\frac{1}{2}m_s}(1,2,3) - \xi^B_c(1,2,3)\chi^{(2)A}_{\frac{1}{2}M_1\frac{1}{2}m_s}(1,2,3)] \tag{A10}$$

where $\xi^A_c(1,2,3)$ and $\xi^B_c(1,2,3)$ are the color octet wave functions given respectively by the Young-Tableau [211] and the Young-Tableau [121] and $\chi^{(2)A}_{\frac{1}{2}M_1\frac{1}{2}m_s}(1,2,3)$ and $\chi^{(2)B}_{\frac{1}{2}M_1\frac{1}{2}m_s}(1,2,3)$ are the corresponding isospin-spin wave functions. Their expressions are

$$\begin{array}{l}\xi_c^A(1,2,3)=\frac{1}{2}\epsilon_{ijb}[q^a(1)q^i(2)q^j(3)+q^a(2)q^i(1)q^j(3)]\\ \xi_c^B(1,2,3)=\frac{1}{2\sqrt{3}}\epsilon_{ijb}[q^a(1)q^i(2)q^j(3)-q^a(2)q^i(1)q^j(3)-2\ q^a(3)q^i(1)q^j(2)]\\ \chi^{(2)A}_{\frac{1}{2}M_1\frac{1}{2}m_s}(1,2,3)=\frac{1}{\sqrt{2}}[\chi^a_{\frac{1}{2}M_1}(1,2,3)\varphi^a_{\frac{1}{2}m_s}(1,2,3)-\chi^b_{\frac{1}{2}M_1}(1,2,3)\varphi^b_{\frac{1}{2}m_s}(1,2,3)]\\ \chi^{(2)B}_{\frac{1}{2}M_1\frac{1}{2}m_s}(1,2,3)=-\frac{1}{\sqrt{2}}[\chi^a_{\frac{1}{2}M_1}(1,2,3)\varphi^b_{\frac{1}{2}m_s}(1,2,3)+\chi^b_{\frac{1}{2}M_1}(1,2,3)\varphi^a_{\frac{1}{2}m_s}(1,2,3)]\end{array} \tag{A11}$$

The second class of the CFS wave function for the K(or $\overline{K}$)-cluster is as follows

$$\Psi^{(2)c}_{\frac{1}{2}M00}(4,5)_K=C^b_a(4,5)\chi_{\frac{1}{2}M}(4,5)\varphi_{00}(4,5) \tag{A12}$$

where

$$C^b_a(4,5)=q^b(4)q_a(5)-\frac{1}{3}\delta^b_a q^c(4)q_c(5) \tag{A13}$$

is the color octet for the $K(\overline{K})$ cluster and the other two functions $\chi_{\frac{1}{2}M}(4,5)$, $\varphi_{00}(4,5)$ are the same as in (A8).

VII. APPENDIX B: THE EFFECTIVE KN AND $\overline{K}N$ INTERACTION POTENTIALS

In this appendix, we show the nonlocal effective interaction potentials of the KN and $\overline{K}N$ systems which are derived from the interquark potentials written in section 2 by the resonating group approach.

The KN nonlocal effective potential $V_t(\vec{R},\vec{R}')$ which is derived from the t-channel OGEP written in Eq. (4) is divided into two parts: the direct part $V_t^D(\vec{R},\vec{R}')$ and the exchanged part $V_t^{ex}(\vec{R},\vec{R}')$:

$$V_t(\vec{R},\vec{R}')=V_t^D(\vec{R},\vec{R}')-V_t^{ex}(\vec{R},\vec{R}') \tag{B1}$$

where

$$V_t^{ex}(\vec{R},\vec{R}')=V_t^{ex}(\vec{R},\vec{R}')^{14}+V_t^{ex}(\vec{R},\vec{R}')^{24}+V_t^{ex}(\vec{R},\vec{R}')^{34} \tag{B2}$$

here the superscript $ab=14,24$ or 34 designates which pair of quarks interchange. Each part of the potential contains several terms as follows:

$$\begin{array}{l}V_t^D(\vec{R},\vec{R}')=V_{15}^D(\vec{R},\vec{R}')+V_{25}^D(\vec{R},\vec{R}')+V_{35}^D(\vec{R},\vec{R}')\\ +V_{14}^D(\vec{R},\vec{R}')+V_{24}^D(\vec{R},\vec{R}')+V_{34}^D(\vec{R},\vec{R}')\end{array} \tag{B3}$$

and

$$\begin{array}{l}V_t^{ex}(\vec{R},\vec{R}')^{ab}=V_{14}^{ex}(\vec{R},\vec{R}')^{ab}+V_{24}^{ex}(\vec{R},\vec{R}')^{ab}+V_{34}^{ex}(\vec{R},\vec{R}')^{ab}+V_{12}^{ex}(\vec{R},\vec{R}')^{ab}+V_{23}^{ex}(\vec{R},\vec{R}')^{ab}\\ +V_{15}^{ex}(\vec{R},\vec{R}')^{ab}+V_{25}^{ex}(\vec{R},\vec{R}')^{ab}+V_{35}^{ex}(\vec{R},\vec{R}')^{ab}+V_{45}^{ex}(\vec{R},\vec{R}')^{ab}+V_{13}^{ex}(\vec{R},\vec{R}')^{ab}\end{array} \tag{B4}$$

where the subscript in each term on the right hand sides (RHS) of (B3) and (B4) marks the two interacting quarks: one in the N-cluster, another in the K-cluster. According to Eq. (25), the terms $V_{ij}^D(\vec{R},\vec{R}')$ and $V_{ij}^{ex}(\vec{R},\vec{R}')^{ab}$ are derived in such a way

$$\begin{array}{c}V_{ij}^D(\vec{R},\vec{R}')=\int d^3\rho d^3\rho'\Gamma(\vec{R},\vec{\rho})V_{ij}^D(\vec{\rho},\vec{\rho}')\Gamma(\vec{\rho}',\vec{R}'),\\ V_{ij}^{ex}(\vec{R},\vec{R}')^{ab}=\int d^3\rho d^3\rho'\Gamma(\vec{R},\vec{\rho})V_{ij}^{ex}(\vec{\rho},\vec{\rho}')^{ab}\Gamma(\vec{\rho}',\vec{R}')\end{array} \tag{B5}$$

in which $V_{ij}^D(\vec{\rho},\vec{\rho}')$ and $V_{ij}^{ex}(\vec{\rho},\vec{\rho}')^{ab}$ can be explicitly calculated according to the definition given in Eq. (20). It should be emphasized that the effective potential in Eq. (23) is defined by the matrix element between the basis wave function written in Eq. (10). In order to exhibit the spin, color and isospin structure of the effective potential, we would like here to give the effective potential in the operator form. The potential operator is derived from the matrix element of the quark potential in Eq. (3) between the position space wave function only, as illustrated in the following:

$$\hat{V}_{ij}^D(\vec{\rho},\vec{\rho}')=\int\prod_{i=1}^5\frac{d^3p_k}{(2\pi)^3}\frac{d^3p_k'}{(2\pi)^3}\langle R(\vec{p}_1,\vec{p}_2,\vec{p}_3,\vec{p}_4,\vec{p}_5;\vec{\rho})\mid V_{ij}^t\mid R(\vec{p}_1,\vec{p}_2,\vec{p}_3,\vec{p}_4,\vec{p}_5;\vec{\rho}')\rangle \tag{B6}$$

and

$$\hat{V}_{ij}^{ex}(\vec{\rho},\vec{\rho}')^{ab}=\int\prod_{i=1}^{5}\frac{d^3p_k}{(2\pi)^3}\frac{d^3p'_k}{(2\pi)^3}\langle R(\vec{p}_1,\vec{p}_2,\vec{p}_3,\vec{p}_4,\vec{p}_5;\vec{\rho})\mid V_{ij}^t P_{ab}\mid R(\vec{p}_1,\vec{p}_2,\vec{p}_3,\vec{p}_4,\vec{p}_5;\vec{\rho}')\rangle \tag{B7}$$

where V_{ij}^t is t-channel OGEP represented in Eq. (4) and $R(\vec{p}_1,\vec{p}_2,\vec{p}_3,\vec{p}_4,\vec{p}_5;\vec{\rho})$ is the position space wave function written in Eq. (14). Clearly, the expressions written in Eq. (24) and ((B1)-(B5) are formally kept unchanged when the potentials in those expressions are replaced by the corresponding operator ones. For instance, when the functions $V_{ij}^D(\vec{\rho},\vec{\rho}')$ and $V_{ij}^{ex}(\vec{\rho},\vec{\rho}')^{ab}$ in (B5) are replaced by the corresponding operators $\hat{V}_{ij}^D(\vec{\rho},\vec{\rho}')$ and $\hat{V}_{ij}^{ex}(\vec{\rho},\vec{\rho}')^{ab}$ defined in (B6) and (B7), through tedious calculations, one may obtain the potential operators $\hat{V}_{ij}^D(\vec{R},\vec{R}')$ and $\hat{V}_{ij}^{ex}(\vec{R},\vec{R}')^{ab}$. The calculated results are displayed below.

First we describe the potential operators which correspond to the ten terms on the RHS of (B4). By introducing the following functions:

$$\begin{aligned}
f_1^t(\vec{R},\vec{R}')_{ex}&=\exp\{-\tfrac{\zeta}{4b^2}[(2\zeta-1)(\vec{R}-\vec{R}')^2+\tfrac{1}{2\zeta-1}(\vec{R}+\vec{R}')^2]\}\\
f_2^t(\vec{R},\vec{R}')_{ex}&=\exp\{-\tfrac{\gamma}{2(3\zeta-2)b^2}[(4\zeta^2-3\zeta+2)\vec{R}^2-8\zeta(\zeta-1)\vec{R}\cdot\vec{R}'+(4\zeta^2-5\zeta+2)\vec{R}'^2]\}\\
f_3^t(\vec{R},\vec{R}')_{ex}&=\exp\{-\tfrac{\zeta(2\zeta-1)}{4b^2}(\vec{R}-\vec{R}')^2-\tfrac{\zeta\cdot(1/2+\alpha_2)}{4b^2(\zeta-1/2-\alpha_2)}(\vec{R}+\vec{R}')^2\}\\
f_4^t(\vec{R},\vec{R}')_{ex}&=\exp\{-\tfrac{\zeta}{2(2\ \zeta-1-\zeta\ \alpha_2)b^2}\{[\zeta(\zeta+\alpha_2)+(\zeta-1)^2]\vec{R}^2+4\zeta(\zeta-1)\vec{R}\cdot\vec{R}'\\
&\quad+[\zeta(\zeta-\alpha_2)+(\zeta-1)^2]\ \vec{R}'^2\}\}
\end{aligned} \tag{B8}$$

with $\zeta=3\beta_2$, the exchanged terms of the potential operator $\hat{V}_t^{ex}(\vec{R},\vec{R}')^{14}$ can be written as

$$\begin{aligned}
\hat{V}_{24}^{ex}(\vec{R},\vec{R}')^{14}&=\tfrac{16\alpha_s C_{24}^t\zeta^3}{\pi^2b^4}(\tfrac{\zeta}{2(2\zeta-1)})^{\frac{3}{2}}f_1^t(\vec{R},\vec{R}')_{ex}\{1-\tfrac{1}{4m_1^2b^2}[\tfrac{9}{4}+3(2\beta_2-1/2)^2+\tfrac{\frac{3}{2}\zeta}{2\zeta-1}+\\
&\tfrac{\zeta^2}{2b^2}\tfrac{4\beta_2-1}{2\zeta-1}(\vec{R}^2-\vec{R}'^2)-\tfrac{\zeta^2}{4b^2(2\zeta-1)^2}(\vec{R}+\vec{R}')^2-\tfrac{\zeta^2}{b^2}(2\beta_2-\tfrac{1}{2})^2(\vec{R}-\vec{R}')^2]\\
&-\tfrac{\zeta^2}{4m_1^2b^4(2\zeta-1)^2}[(\zeta-1)\vec{R}'-\zeta\vec{R}]^2+\tfrac{3\zeta}{8m_1^2b^2(2\zeta-1)}+\tfrac{3}{4m_1^2b^2}-i\tfrac{\zeta^2}{4m_1^2b^4(2\zeta-1)}(1+\gamma)(\vec{R}\times\vec{R}')\cdot(\vec{\sigma}_2-\vec{\sigma}_4)\\
&+\tfrac{1}{4m_1^2}[(\tfrac{\gamma}{b^2}+\tfrac{\gamma^2}{4b^2}\tfrac{2\zeta}{2\zeta-1})\vec{\sigma}_2\cdot\vec{\sigma}_4-\tfrac{\gamma^2\zeta^2}{4b^4(2\zeta-1)^2}(\zeta\vec{R}-(\zeta-1)\vec{R}')\cdot\vec{\sigma}_2(\zeta\vec{R}-(\zeta-1)\vec{R}')]\}\\
&-\tfrac{4\alpha_s C_{24}^t\gamma^3}{\pi^2m_1^2b^6}(\tfrac{\zeta}{3\zeta-1})^{\frac{3}{2}}f_2^t(\vec{R},\vec{R}')_{ex}(1+\vec{\sigma}_2\cdot\vec{\sigma}_4),
\end{aligned} \tag{B9}$$

$$\begin{aligned}
\hat{V}_{25}^{ex}(\vec{R},\vec{R}')^{14}&=\tfrac{8\alpha_s C_{25}^t\zeta^3}{\alpha_2\pi^2b^4}(\tfrac{\beta_1}{2\zeta-1})^{\frac{3}{2}}f_1^t(\vec{R},\vec{R}')_{ex}\{1-\tfrac{1}{m_{12}^2b^2}[\tfrac{3}{2\alpha_1}+3\tfrac{(\alpha_1-\beta_1)^2}{\alpha_1^2}-\tfrac{(\alpha_1-\beta_1)^2\zeta^2}{\alpha_1^2b^2}(\vec{R}-\vec{R}')^2]\\
&+\tfrac{m_1-m_2}{m_1m_2m_{12}b^2}[\tfrac{3(\alpha_1-\beta_1)}{\alpha}-\tfrac{(\alpha_1-\beta_1)\ \zeta^2}{\alpha\ b^2}(\vec{R}-\vec{R}')^2]-i\tfrac{(\alpha_1-\beta_1)\ \zeta^2}{2m_{12}\alpha\ b^4(2\zeta-1)}(1+\gamma)(\vec{R}\times\vec{R}')\cdot(\tfrac{\vec{\sigma}_2}{m_1}-\tfrac{\vec{\sigma}_5}{m_2})\\
&+i\tfrac{(\alpha_1-\beta_1)\ \zeta^2\alpha_2^2}{2m_1m_2\ b^4(2\zeta-1)}(1+\gamma)(\vec{R}\times\vec{R}')\cdot[(2+\tfrac{m_2}{m_1})\vec{\sigma}_2-(2+\tfrac{m_1}{m_2})\vec{\sigma}_5]\\
&+\tfrac{1}{4m_1m_2}[(\tfrac{2\alpha_2\gamma}{b^2}+\tfrac{\gamma^2}{b^2}\tfrac{4\alpha_2^2}{2\zeta-1})\vec{\sigma}_2\cdot\vec{\sigma}_5-\tfrac{4\gamma^2\zeta^2\alpha_2^2}{b^4(2\zeta-1)^2}(\vec{R}+\vec{R}')\cdot\vec{\sigma}_2(\vec{R}+\vec{R}')\cdot\vec{\sigma}_5]\}\\
&-\tfrac{16\alpha_s C_{25}^t\zeta^3}{\pi^2b^6}(\tfrac{\beta_1}{2(\zeta-\frac{1}{2}-\alpha_2)})^{\frac{3}{2}}f_3^t(\vec{R},\vec{R}')_{ex}\tfrac{1}{4m_1m_2}(\tfrac{m_1^2+m_2^2}{2m_1m_2}+\vec{\sigma}_2\cdot\vec{\sigma}_5),
\end{aligned} \tag{B10}$$

$$\begin{aligned}
\hat{V}_{15}^{ex}(\vec{R},\vec{R}')^{14}&=\tfrac{8\alpha_s C_{15}^t\zeta^3}{\alpha_2\pi^2b^4}(\tfrac{\beta_1}{2\zeta-1})^{\frac{3}{2}}f_1^t(\vec{R},\vec{R}')_{ex}\{1-\tfrac{1}{m_{12}^2b^2}[\tfrac{\zeta}{2\alpha_1}+\tfrac{3\ \zeta}{2}(2\ \zeta-1+\tfrac{1}{2\ \zeta-1})\\
&-\tfrac{\zeta^2}{4(2\ \zeta-1)^2b^2}([(2\ \zeta-1)^2-1]\vec{R}-[(2\ \zeta-1)^2+1]\vec{R}')^2]+\tfrac{\alpha_2(m_1-m_2)}{4m_1m_2m_{12}b^2(2\ \zeta-1)}[-12\zeta(\zeta-1)\\
&-\tfrac{2\ \zeta^2}{b^2(2\ \zeta-1)}((\zeta-1)\vec{R}-\zeta\vec{R}')([(2\zeta-1)^2-1]\vec{R}-[(2\zeta-1)^2+1]\vec{R}')]+\tfrac{1}{4m_1m_2b^2}[6\alpha_2(1+\tfrac{\alpha_2\zeta}{2\zeta-1})\\
&-\tfrac{4\zeta^2\alpha_2^2}{b^2(2\ \zeta-1)^2}((2\zeta+1)\vec{R}-(2\zeta-3)\vec{R}')^2]+i\tfrac{\beta_1\zeta^2}{2m_{12}\alpha\ b^4(2\zeta-1)}(1+\gamma)(\vec{R}\times\vec{R}')\cdot(\tfrac{\vec{\sigma}_1}{m_1}-\tfrac{\vec{\sigma}_5}{m_2})\\
&+\tfrac{1}{4m_1m_2}[(\tfrac{2\alpha_2\gamma}{b^2}+\tfrac{\gamma^2}{b^2}\tfrac{2\zeta\alpha_2^2}{2\zeta-1})\vec{\sigma}_1\cdot\vec{\sigma}_5-\tfrac{4\gamma^2\zeta^2\alpha_2^2}{b^4(2\zeta-1)^2}(\varsigma\vec{R}-(\zeta-1)\vec{R}')\cdot\vec{\sigma}_1(\varsigma\vec{R}-(\zeta-1)\vec{R}')\cdot\vec{\sigma}_5]\}\\
&-\tfrac{16\alpha_s C_{15}^t\zeta^3}{\pi^2b^6}(\tfrac{\beta_1}{2\zeta-1-\zeta\alpha_2)})^{\frac{3}{2}}f_4^t(\vec{R},\vec{R}')_{ex}\tfrac{1}{4m_1m_2}(\tfrac{m_1^2+m_2^2}{2m_1m_2}+\vec{\sigma}_1\cdot\vec{\sigma}_5),
\end{aligned} \tag{B11}$$

$$\begin{aligned}
\hat{V}_{14}^{ex}(\vec{R},\vec{R}')^{14}&=\tfrac{16\alpha_s C_{14}^t\zeta^3}{\pi^2b^4}(\tfrac{\zeta}{2(2\zeta-1)})^{\frac{3}{2}}f_1^t(\vec{R},\vec{R}')_{ex}\{1-\tfrac{1}{4m_1^2b^2}[3+3(\beta_2-\beta_1)^2-\tfrac{\zeta^2(\beta_2-\beta_1)^2}{b^2}(\vec{R}-\vec{R}')^2]\\
&+\tfrac{1}{4m_1^2b^2}[3+\tfrac{12}{2\zeta-1}-\tfrac{4\ \zeta^2}{b^2(2\zeta-1)^2}(\vec{R}+\vec{R}')^2]-i\tfrac{3\zeta^2}{4m_1^2b^4(2\zeta-1)}(1+\gamma)(\vec{R}\times\vec{R}')\cdot(\vec{\sigma}_1+\vec{\sigma}_4)\\
&+\tfrac{1}{4m_1^2b^2}[(\gamma+\gamma^2)\vec{\sigma}_1\cdot\vec{\sigma}_4-\tfrac{\gamma^2\zeta^2}{b^2}(\vec{R}-\vec{R}')\cdot\vec{\sigma}_1(\vec{R}-\vec{R}')\cdot\vec{\sigma}_4]\}\\
&-\tfrac{\alpha_s C_{14}^t}{\pi^2m_1^2b^3}(\tfrac{\pi\ \zeta}{2\zeta-1})^{\frac{3}{2}}\delta(\vec{R}-\vec{R}')e^{-\frac{\zeta}{4\ b^2(2\zeta-1)}(\vec{R}+\vec{R}')^2}(1+\vec{\sigma}_1\cdot\vec{\sigma}_4),
\end{aligned} \tag{B12}$$

$$\hat{V}_{34}^{ex}(\vec{R},\vec{R}')^{14} = \frac{16\alpha_s C_{34}^t\zeta^3}{\pi^2 b^4}(\frac{\zeta}{2(2\zeta-1)})^{\frac{3}{2}} f_1^t(\vec{R},\vec{R}')_{ex}\{1-\frac{1}{4m_1^2b^2}[3+3(\beta_2-\beta_1)^2-\frac{\zeta^2(\beta_2-\beta_1)^2}{b^2}(\vec{R}-\vec{R}')^2]$$
$$+\frac{1}{4m_1^2b^2}[3+\frac{12}{2\zeta-1}-\frac{4\ \zeta^2}{b^2(2\zeta-1)^2}(\vec{R}+\vec{R}')^2]-i\frac{3\zeta^2}{4m_1^2b^4(2\zeta-1)}(1+\gamma)(\vec{R}\times\vec{R}')\cdot(\vec{\sigma}_3+\vec{\sigma}_4)$$
$$+\frac{1}{4m_1^2b^2}[(\gamma+\gamma^2)\vec{\sigma}_3\cdot\vec{\sigma}_4-\frac{\gamma^2\zeta^2}{b^2}(\vec{R}-\vec{R}')\cdot\vec{\sigma}_3(\vec{R}-\vec{R}')\cdot\vec{\sigma}_4]\}$$
$$-\frac{\alpha_s C_{34}^t}{\pi^2 m_1^2 b^3}(\frac{\pi\ \zeta}{2\zeta-1})^{\frac{3}{2}}\delta(\vec{R}-\vec{R}')e^{-\frac{\zeta}{4\ b^2(2\zeta-1)}(\vec{R}+\vec{R}')^2}(1+\vec{\sigma}_3\cdot\vec{\sigma}_4) \tag{B13}$$

$$\hat{V}_{12}^{ex}(\vec{R},\vec{R}')^{14} = \frac{16\alpha_s C_{12}^t\zeta^3}{\pi^2 b^4}(\frac{\zeta}{2(2\zeta-1)})^{\frac{3}{2}} f_1^t(\vec{R},\vec{R}')_{ex}\{1-\frac{1}{4m_1^2b^2}[3+3(\beta_2-\beta_1)^2-\frac{\zeta^2(\beta_2-\beta_1)^2}{b^2}(\vec{R}-\vec{R}')^2]$$
$$+\frac{1}{4m_1^2b^2}[3+\frac{12}{2\zeta-1}-\frac{4\ \zeta^2}{b^2(2\zeta-1)^2}(\vec{R}+\vec{R}')^2]+i\frac{3\zeta^2}{4m_1^2b^4(2\zeta-1)}(1+\gamma)(\vec{R}\times\vec{R}')\cdot(\vec{\sigma}_1+\vec{\sigma}_2)$$
$$+\frac{1}{4m_1^2b^2}[(\gamma+\gamma^2)\vec{\sigma}_1\cdot\vec{\sigma}_2-\frac{\gamma^2\zeta^2}{b^2}(\vec{R}-\vec{R}')\cdot\vec{\sigma}_1(\vec{R}-\vec{R}')\cdot\vec{\sigma}_2]\}$$
$$-\frac{\alpha_s C_{12}^t}{\pi^2 m_1^2 b^3}(\frac{\pi\ \zeta}{2\zeta-1})^{\frac{3}{2}}\delta(\vec{R}-\vec{R}')e^{-\frac{\zeta}{4\ b^2(2\zeta-1)}(\vec{R}+\vec{R}')^2}(1+\vec{\sigma}_1\cdot\vec{\sigma}_2), \tag{B14}$$

$$\hat{V}_{13}^{ex}(\vec{R},\vec{R}')^{14} = \frac{16\alpha_s C_{13}^t\zeta^3}{\pi^2 b^4}(\frac{\zeta}{2(2\zeta-1)})^{\frac{3}{2}} f_1^t(\vec{R},\vec{R}')_{ex}\{1-\frac{1}{4m_1^2b^2}[3+3(\beta_2-\beta_1)^2-\frac{\zeta^2(\beta_2-\beta_1)^2}{b^2}(\vec{R}-\vec{R}')^2]$$
$$+\frac{1}{4m_1^2b^2}[3+\frac{12}{2\zeta-1}-\frac{4\ \zeta^2}{b^2(2\zeta-1)^2}(\vec{R}+\vec{R}')^2]+i\frac{3\zeta^2}{4m_1^2b^4(2\zeta-1)}(1+\gamma)(\vec{R}\times\vec{R}')\cdot(\vec{\sigma}_1+\vec{\sigma}_3)$$
$$+\frac{1}{4m_1^2b^2}[(\gamma+\gamma^2)\vec{\sigma}_1\cdot\vec{\sigma}_3-\frac{\gamma^2\zeta^2}{b^2}(\vec{R}-\vec{R}')\cdot\vec{\sigma}_1(\vec{R}-\vec{R}')\cdot\vec{\sigma}_3]\}$$
$$-\frac{\alpha_s C_{13}^t}{\pi^2 m_1^2 b^3}(\frac{\pi\ \zeta}{2\zeta-1})^{\frac{3}{2}}\delta(\vec{R}-\vec{R}')e^{-\frac{\zeta}{4\ b^2(2\zeta-1)}(\vec{R}+\vec{R}')^2}(1+\vec{\sigma}_1\cdot\vec{\sigma}_3), \tag{B15}$$

$$\hat{V}_{23}^{ex}(\vec{R},\vec{R}')^{14} = \frac{16\alpha_s C_{23}^t\zeta^3}{\pi^2 b^4}(\frac{\zeta}{2(2\zeta-1)})^{\frac{3}{2}} f_1^t(\vec{R},\vec{R}')_{ex}\{1-\frac{1}{4m_1^2b^2}[3+12\ \beta_2^2$$
$$-\frac{4\ \beta_2^2\zeta^2}{b^2}(\vec{R}^2-\vec{R}'^2)]+\frac{1}{2m_1^2b^2}-\frac{1}{6m_1^2b^2}\vec{\sigma}_2\cdot\vec{\sigma}_3\}, \tag{B16}$$

$$\hat{V}_{35}^{ex}(\vec{R},\vec{R}')^{14} = \frac{8\alpha_s C_{35}^t\zeta^3}{\alpha_2\pi^2 b^4}(\frac{\beta_1}{2\zeta-1})^{\frac{3}{2}} f_1^t(\vec{R},\vec{R}')_{ex}\{1-\frac{1}{m_{12}^2b^2}[\frac{3}{2\alpha_1}+3\frac{(\alpha_1-\beta_1)^2}{\alpha_1^2}-\frac{(\alpha_1-\beta_1)^2\zeta^2}{\alpha_1^2b^2}(\vec{R}-\vec{R}')^2]$$
$$+\frac{m_1-m_2}{m_1m_2m_{12}b^2}[\frac{3(\alpha_1-\beta_1)}{\alpha}-\frac{(\alpha_1-\beta_1)\ \zeta^2}{\alpha\ b^2}(\vec{R}-\vec{R}')^2]-i\frac{(\alpha_1-\beta_1)\ \zeta^2}{2m_{12}\alpha\ b^4(2\zeta-1)}(1+\gamma)(\vec{R}\times\vec{R}')\cdot(\frac{\vec{\sigma}_3}{m_1}-\frac{\vec{\sigma}_5}{m_2})$$
$$+i\frac{(\alpha_1-\beta_1)\ \zeta^2\alpha_2^2}{2m_1m_2\ b^4(2\zeta-1)}(1+\gamma)(\vec{R}\times\vec{R}')\cdot[(2+\frac{m_2}{m_1})\vec{\sigma}_3-(2+\frac{m_1}{m_2})\vec{\sigma}_5]$$
$$+\frac{1}{4m_1m_2}[(\frac{2\alpha_2\gamma}{b^2}+\frac{\gamma^2}{b^2}\frac{4\alpha_2^2}{2\zeta-1})\vec{\sigma}_3\cdot\vec{\sigma}_5-\frac{4\gamma^2\zeta^2\alpha_2^2}{b^4(2\zeta-1)^2}(\vec{R}+\vec{R}')\cdot\vec{\sigma}_3(\vec{R}+\vec{R}')\cdot\vec{\sigma}_5]\}$$
$$-\frac{16\alpha_s C_{35}^t\zeta^3}{\pi^2 b^6}(\frac{\beta_1}{2(\zeta-\frac{1}{2}-\alpha_2)})^{\frac{3}{2}} f_3^t(\vec{R},\vec{R}')_{ex}\frac{1}{4m_1m_2}(\frac{m_1^2+m_2^2}{2m_1m_2}+\vec{\sigma}_3\cdot\vec{\sigma}_5) \tag{B17}$$

and

$$\hat{V}_{45}^{ex}(\vec{R},\vec{R}')^{14} = \frac{8\alpha_s C_{45}^t\zeta^3}{\alpha_2\pi^2 b^4}(\frac{\beta_1}{2\zeta-1})^{\frac{3}{2}} f_1^t(\vec{R},\vec{R}')_{ex}\{1-\frac{1}{m_{12}^2b^2}[\frac{\zeta}{2\alpha_1}+\frac{3\ \zeta}{2}(2\ \zeta-1+\frac{1}{2\ \zeta-1})$$
$$-\frac{\zeta^2}{4(2\ \zeta-1)^2b^2}([(2\ \zeta-1)^2-1]\vec{R}'-[(2\ \zeta-1)^2+1]\vec{R})^2]+\frac{\alpha_2(m_1-m_2)}{4m_1m_2m_{12}b^2(2\ \zeta-1)}[-12\zeta(\zeta-1)$$
$$-\frac{2\ \zeta^2}{b^2(2\ \zeta-1)}((\zeta-1)\vec{R}'-\zeta\vec{R})([(2\zeta-1)^2-1]\vec{R}'-[(2\zeta-1)^2+1]\vec{R})]+\frac{1}{4m_1m_2b^2}[6\alpha_2(1+\frac{\alpha_2\zeta}{2\zeta-1})$$
$$-\frac{4\zeta^2\alpha_2^2}{b^2(2\ \zeta-1)^2}((2\zeta+1)\vec{R}'-(2\zeta-3)\vec{R})^2]-i\frac{\beta_1\zeta^2}{2m_{12}\alpha\ b^4(2\zeta-1)}(1+\gamma)(\vec{R}\times\vec{R}')\cdot(\frac{\vec{\sigma}_4}{m_1}-\frac{\vec{\sigma}_5}{m_2})$$
$$+\frac{1}{4m_1m_2}[(\frac{2\alpha_2\gamma}{b^2}+\frac{\gamma^2}{b^2}\frac{2\zeta\alpha_2^2}{2\zeta-1})\vec{\sigma}_4\cdot\vec{\sigma}_5-\frac{4\gamma^2\zeta^2\alpha_2^2}{b^4(2\zeta-1)^2}(\zeta\vec{R}'-(\zeta-1)\vec{R})\cdot\vec{\sigma}_4(\zeta\vec{R}'-(\zeta-1)\vec{R}\cdot\vec{\sigma}_5]\}$$
$$-\frac{16\alpha_s C_{45}^t\zeta^3}{\pi^2 b^6}(\frac{\beta_1}{2\zeta-1-\zeta\alpha_2})^{\frac{3}{2}} f_4^t(\vec{R},\vec{R}')_{ex}\frac{1}{4m_1m_2}(\frac{m_1^2+m_2^2}{2m_1m_2}+\vec{\sigma}_4\cdot\vec{\sigma}_5) \tag{B18}$$

in which $\alpha_1=\frac{m_1}{m_1+m_2},\alpha_2=\frac{m_2}{m_1+m_2}$. The other exchanged potential operators $\hat{V}_t^{ex}(\vec{R},\vec{R}')^{24}$ and $\hat{V}_t^{ex}(\vec{R},\vec{R}')^{34}$ can directly be written out from the above operators by changing the superscripts 14 to 24 and 34.

The potential operators corresponding to the terms of the direct part of the potential in (B3) are shown in the following

$$\hat{V}_{24}^{D}(\vec{R},\vec{R}') = \frac{16\pi\alpha_s C_{24}^d}{b}(\frac{\zeta}{\pi\ (2\zeta-\gamma)})^{\frac{3}{2}}\delta(\vec{R}-\vec{R}')e^{-\frac{\gamma\ \zeta}{b^2(2\zeta-\gamma)}\vec{R}^2}\{1-\frac{1}{4m_1^2b^2}[3-\frac{3}{4}(\beta_2-\beta_1)^2(\frac{1}{2\zeta}+\frac{1}{\gamma})$$
$$-b^2((\frac{1}{2\zeta}+\frac{1}{\gamma})\nabla_{\vec{R}}-(\frac{1}{2\zeta}-\frac{1}{\gamma})\nabla_{\vec{R}'})^2]+\frac{1}{4m_1^2b^2}[3(1-\frac{1}{\gamma})-\frac{b^2}{\gamma^2}(\nabla_{\vec{R}}-\nabla_{\vec{R}'})^2]$$
$$-i\frac{1}{8m_1^2b^2}\frac{2(\beta_2-\beta_1)}{2\zeta-\lambda}(1+\gamma)(\vec{\sigma}_2-\vec{\sigma}_4)\cdot(\vec{R}\times\nabla_{\vec{R}})+i\frac{3}{4m_1^2b^2(2\zeta-\lambda)}(1+\gamma)(\vec{\sigma}_2+\vec{\sigma}_4)\cdot(\vec{R}\times\nabla_{\vec{R}})$$
$$+\frac{1}{4m_1^2b^2}[\frac{2\zeta\ \lambda}{2\zeta-\lambda}\vec{\sigma}_2\cdot\vec{\sigma}_4-\frac{4\gamma^2\zeta^2}{b^2(2\zeta-\gamma)^2}\vec{R}\cdot\vec{\sigma}_2\vec{R}\cdot\vec{\sigma}_4]\}$$
$$-\frac{1}{4m_1^2}\frac{16\alpha_s C_{24}^d}{\pi^2b^3}(\frac{\pi\ \zeta}{2\zeta-1})^{\frac{3}{2}}\delta(\vec{R}-\vec{R}')e^{-\frac{\zeta}{b^2(2\zeta-1)}\vec{R}^2}\vec{\sigma}_2\cdot\vec{\sigma}_4. \tag{B19}$$

The potential operators corresponding to the terms $V_{14}^D(\vec{R},\vec{R}')$ and $V_{34}^D(\vec{R},\vec{R}')$ in (B3) have the same form as shown above except for the subscripts 24 being changed to 14 and 34. Introducing

$$f_5^t(\vec{R},\vec{R}')_D = \exp\{-\frac{1}{\zeta_1 b^2(1-\frac{\zeta_2^2}{\zeta_1^2})}(\vec{R}^2+2\frac{\zeta_2}{\zeta_1}\vec{R}\cdot\vec{R}'+\vec{R}'^2)\} \tag{B20}$$

with $\zeta_1 = 1/(\zeta-\beta_1^2)+1/\gamma\alpha_2-2/\varsigma$ and $\zeta_2 = 1/(\zeta-\beta_1^2)+1/\gamma\alpha_2$ and

$$f_6^t(\vec{R},\vec{R}')_D = \exp\{-\frac{1}{\zeta_1' b^2(1-\frac{\zeta_2'^2}{\zeta_1'^2})}(\vec{R}^2+2\frac{\zeta_2'}{\zeta_1'}\vec{R}\cdot\vec{R}'+\vec{R}'^2)\} \tag{B21}$$

with $\zeta_1' = 1/(\zeta-\beta_1^2)+1/\alpha_2-2/\varsigma$ and and $\zeta_2' = 1/(\zeta-\beta_1^2)+1/\alpha_2$, the potential operator corresponding to the term $V_{25}^D(\vec{R},\vec{R}')$ in (B3) can be represented in the form

$$\begin{aligned}
\hat{V}_{25}^D(\vec{R},\vec{R}') = {}& \tfrac{8\alpha_s C_{25}^d}{\pi^2\alpha_2\zeta_1^3 b^4}(\tfrac{\alpha\ \zeta}{\gamma(\zeta^2-\beta_1^2)(1-\frac{\zeta_2^2}{\zeta_1^2})})^{\frac{3}{2}} f_5^t(\vec{R},\vec{R}')_D\{1-\tfrac{1}{m_{12}^2b^2}[\tfrac{3}{2\alpha_1}+\tfrac{(\alpha_1-\beta_1)^2}{4\alpha_1^2}(-\tfrac{6}{\zeta-\beta_1^2}+ \\
& \tfrac{12}{(\zeta-\beta_1^2)^2\zeta_1(1+\frac{\zeta_2}{\zeta_1})})-\tfrac{(\alpha_1-\beta_1)^2}{4\alpha_1^2b^2}\tfrac{4}{(\zeta-\beta_1^2)^2(\zeta_1+\zeta_2)^2}(\vec{R}-\vec{R}')^2]+\tfrac{m_1-m_2}{4m_1m_2m_{12}b^4}\alpha_2(\beta_2-\tfrac{\beta_1}{\alpha})[(-\tfrac{6}{\zeta-\beta_1^2} \\
& +\tfrac{12}{(\zeta-\beta_1^2)^2\zeta_1(1+\frac{\zeta_2}{\zeta_1})})b^2-\tfrac{4}{(\zeta-\beta_1^2)^2(\zeta_1+\zeta_2)^2}(\vec{R}-\vec{R}')^2)]+\tfrac{1}{4m_1m_2}[\tfrac{6\alpha_2}{b^2}+\tfrac{\alpha_2^2}{b^4}((-\tfrac{6}{\zeta-\beta_1^2}+\tfrac{12}{(\zeta-\beta_1^2)^2\zeta_1(1+\frac{\zeta_2}{\zeta_1})})b^2 \\
& -\tfrac{4}{(\zeta-\beta_1^2)^2(\zeta_1+\zeta_2)^2}(\vec{R}-\vec{R}')^2)]-i\tfrac{4\ (\alpha_1-\beta_1)}{4m_{12}\alpha_1\ (\zeta-\beta_1^2)b^4(\zeta_1^2-\zeta_2^2)}(1+\gamma)(\vec{R}\times\vec{R}')\cdot(\tfrac{\vec{\sigma}_2}{m_1}-\tfrac{\vec{\sigma}_5}{m_2}) \\
& +i\tfrac{4\alpha_2}{4m_1m_2\ (\zeta-\beta_1^2)b^4(\zeta_1^2-\zeta_2^2)}(1+\gamma)(\vec{R}\times\vec{R}')\cdot[(2+\tfrac{m_2}{m_1})\vec{\sigma}_2-(2+\tfrac{m_1}{m_2})\vec{\sigma}_5] \\
& +\tfrac{1}{4m_1m_2}[\tfrac{4}{b^2(\zeta_1-\zeta_2)}\vec{\sigma}_2\cdot\vec{\sigma}_5-\tfrac{4}{b^4(\zeta_1-\zeta_2)^2}(\vec{R}+\vec{R}')\cdot\vec{\sigma}_2(\vec{R}+\vec{R}')\cdot\vec{\sigma}_5]\} \\
& -\tfrac{8\alpha_s C_{25}^d}{\pi^2\alpha_2\zeta_1'^3 b^4}(\tfrac{\alpha\ \zeta}{(\zeta^2-\beta_1^2)(1-\frac{\zeta_2'^2}{\zeta_1'^2})})^{\frac{3}{2}} f_6^t(\vec{R},\vec{R}')_D\tfrac{1}{4m_1m_2}(\tfrac{m_1^2+m_2^2}{2m_1^2m_2^2}+\vec{\sigma}_2\cdot\vec{\sigma}_5).
\end{aligned} \tag{B22}$$

The potential operators corresponding to the remaining two terms in (B3) are of the same form as shown above except for the subscripts 25 being replaced by 15 and 35.

Let us turn to the $\overline{K}N$ interaction potential. For the $\overline{K}N$ interaction, the effective potential coming from the t-channel OGEP only has a direct part as represented in (B3) and (B19)-(B22) because there are no identical particles between the N-cluster (qqq) and the $\overline{K}$-cluster ($\overline{q}s$). Besides, the nonlocal effective potential derived from the s-channel OGEP must be considered and plays an essential role in the $\overline{K}N$ interaction. This potential can be written as

$$V^s(\vec{R},\vec{R}') = V_{14}^{s\text{-}d}(\vec{R},\vec{R}')+V_{24}^{s\text{-}d}(\vec{R},\vec{R}')+V_{34}^{s\text{-}d}(\vec{R},\vec{R}') \tag{B23}$$

where $V_{ij}^{s\text{-}d}(\vec{R},\vec{R}')$ denotes the direct term of the potential generated from the interaction between the quark i and the antiquark j. The corresponding operator form of the potentials on the RHS of (B23) can be derived in the same way as shown before for the t-channel potential operators. The results are

$$\begin{aligned}
\hat{V}_{14}^{s\text{-}d}(\vec{R},\vec{R}') = {}& \tfrac{\pi\alpha_s F_{14}^a C_{14}^s}{2m_1^2(2\pi b^2)^{3/2}}(\tfrac{2\zeta}{2\zeta-1})^{\frac{3}{2}}\delta(\vec{R}-\vec{R}')e^{-\frac{\zeta}{4\ b^2(2\zeta-1)}(\vec{R}+\vec{R}')^2}\{(3+\vec{\sigma}_1\cdot\vec{\sigma}_4) \\
& -\tfrac{1}{4m_1^2b^2}[3-\tfrac{3(\beta_2-\beta_1)^2}{2\zeta}+\tfrac{3\ (\beta_2-\beta_1)^2}{\zeta\ (2\zeta-1)}-\tfrac{2\ (\beta_2-\beta_1)^2}{\zeta(2\zeta-1)^2b^2}\vec{R}^2+\tfrac{4\ (\beta_2-\beta_1)^2}{(2\zeta-1)\zeta}\vec{R}\cdot\nabla_{\vec{R}}+b^2\nabla_{\vec{R}}^2]\cdot(3+\vec{\sigma}_1\cdot\vec{\sigma}_4) \\
& -\tfrac{1}{2m_1^2b^2}[3-6(\tfrac{1}{4\zeta}-\tfrac{\zeta}{2\zeta-1})+\tfrac{\zeta^2}{b^2\ (2\zeta-1)^2}(\vec{R}+\vec{R}')^2+\tfrac{3}{\zeta\ (2\zeta-1)}-\tfrac{2}{(2\zeta-1)^2b^2}\vec{R}^2 \\
& +\tfrac{4}{(2\zeta-1)\zeta}\vec{R}\cdot\nabla_{\vec{R}}-\tfrac{2b^2}{\zeta^2}\nabla_{\vec{R}}^2]\cdot(2+\vec{\sigma}_1\cdot\vec{\sigma}_4)-i\tfrac{\beta_2-\beta_1}{m_1^2b^2(2\zeta-1)}(\vec{\sigma}_1-\vec{\sigma}_4)\cdot(\vec{R}\times\nabla_{\vec{R}}) \\
& +\tfrac{1}{2m_1^2b^2}[-\tfrac{2\zeta}{2\zeta-1}\vec{\sigma}_1\cdot\vec{\sigma}_4+\tfrac{1}{4b^2(2\zeta-1)^2}(\vec{R}+\vec{R}')\cdot\vec{\sigma}_1(\vec{R}+\vec{R}')\cdot\vec{\sigma}_4+\tfrac{4\zeta}{2\zeta-1}\vec{\sigma}_1\cdot\vec{\sigma}_4 \\
& -\tfrac{8\zeta^2}{(2\zeta-1)^2b^2}\vec{R}\cdot\vec{\sigma}_1\vec{R}\cdot\vec{\sigma}_4+\tfrac{16\zeta}{2\zeta-1}\vec{R}\cdot\vec{\sigma}_1\nabla_{\vec{R}}\cdot\vec{\sigma}_4+8b^2\ \nabla_{\vec{R}}\cdot\vec{\sigma}_1\nabla_{\vec{R}}\cdot\vec{\sigma}_4]\}.
\end{aligned} \tag{B24}$$

The other two terms $\hat{V}_{24}^{s\text{-}d}(\vec{R},\vec{R}')$ and $\hat{V}_{34}^{s\text{-}d}(\vec{R},\vec{R}')$ can be written out from the above expression by the substitution of the subscripts 24 and 34 for 14.

The effective KN ($\overline{K}N$) potential derived from the interquark harmonic oscillator confining potential and quark interchanges is of a simple expression whose operator form is represented as

$$\begin{aligned}
\hat{V}_c^{ex}(\vec{R},\vec{R}') = {}& -12b^2\omega^2\{C_s^{24}\mu_{24}+C_s^{34}\mu_{34}+C_s^{12}\mu_{12}+C_s^{13}\mu_{13}+C_s^{14}\mu_{14} \\
& +\tfrac{1}{2\alpha_2}[C_s^{25}\mu_{25}+C_s^{35}\mu_{35}+C_s^{15}\mu_{15}+C_s^{45}\mu_{45}]\}4(\tfrac{\zeta}{\pi})^3(\tfrac{\pi\zeta}{(2\zeta-1)b^2})^{\frac{3}{2}}e^{-\frac{\zeta(2\zeta-1)}{4b^2}(\vec{R}-\vec{R}')^2-\frac{\zeta}{4b^2(2\zeta-1)}(\vec{R}+\vec{R}')^2}
\end{aligned} \tag{B25}$$

where μ_{ij} denotes the reduced mass of interacting quarks i and j and the color factors are the same as the ones appearing in the t-channel effective potentials.

Apart from the potentials listed above, there are additional terms in the KN and $\overline{K}N$ potentials occurring in the resonating group equation which arise from the kinetic term and the normalization term in the resonating group equation due to the effect of quark rearrangement. They are respectively written in the following:

$$\begin{array}{c} T^{ex}(\vec{R},\vec{R}') = (-3)\alpha^{3/2}\{\frac{1}{2\mu}[\frac{\zeta}{2b^2} - \frac{(\zeta\,\vec{R}-\zeta\,\vec{R}'+\vec{R}')^2}{4b^4}] + \frac{1}{2\mu_1}[\frac{3}{4b^2} - \frac{\vec{R}'^2}{16b^4}] \\ +\frac{1}{2\mu_2}[\frac{1}{4b^2} - \frac{\vec{R}'^2}{144b^4}] + \frac{1}{2\mu_3}[\frac{3\alpha_2}{2\,b^2} - \frac{\alpha_2^2\vec{R}'^2}{4b^4}]\} f_T^{ex}(\vec{R},\vec{R}') \end{array} \tag{B26}$$

where

$$\begin{array}{c} f_T^{ex}(\vec{R},\vec{R}') = 4\zeta^3(\frac{\zeta}{\pi b^2(2\zeta-1)(2\zeta-\frac{2}{\frac{1}{3}+\alpha_1}+1)})^{\frac{3}{2}} \\ \times \exp\{-\frac{\zeta(\frac{2}{\frac{1}{3}+\alpha_1}-1)}{4b^2(2\zeta-\frac{2}{\frac{1}{3}+\alpha_1}+1)}(\vec{R}-\vec{R}')^2 - \frac{\zeta}{4b^2(2\zeta-1)}(\vec{R}+\vec{R}')^2\}, \end{array} \tag{B27}$$

with

$$\mu = \frac{3m_1(m_1+m_2)}{4m_1+m_2}, \mu_1 = \frac{m_1}{2}, \mu_2 = \frac{2m_1}{3}, \mu_3 = \frac{m_1m_2}{m_1+m_2}, \gamma_1 = 3/(1/3+\alpha_1). \tag{B28}$$

and

$$N^{ex}(\vec{R},\vec{R}') = -3E_r^{\frac{3}{2}}\exp\{-\frac{\zeta(-2\beta_1^2-2\beta_2^2-1)}{4b^2(2\zeta-2\beta_1^2-2\beta_2^2+1)}(\vec{R}-\vec{R}')^2 - \frac{\zeta}{4b^2(2\zeta-1)}(\vec{R}+\vec{R}')^2\} \tag{B29}$$

here E_r is the relative energy of two clusters.

The effective potential in Eq. (23) is given by the color-spin-isospin matrix element of the above potential operator

$$V(\vec{R},\vec{R}') = \langle\Psi_{TM\frac{1}{2}m}(1,2,3,4,5) \mid \hat{V}(\vec{R},\vec{R}') \mid \Psi_{TM\frac{1}{2}m}(1,2,3,4,5) \tag{B30}$$

where $\hat{V}(\vec{R},\vec{R}')$ has the expression as written in Eq. (24) and in this appendix and $\Psi_{TM\frac{1}{2}m}(1,2,3,4,5)$ is the color-spin-isospin wave function represented in Eq. (12) and Appendix A.

To incorporate the QCD renormalization effect into the model, the QCD fine structure constant α_s and quark masses in the potential operators will be replaced by their effective ones. The effective fine structure constant derived in the one-loop approximation has the expression like this [40]

$$\alpha_s(\lambda) = \frac{\alpha_s^0}{1+\frac{\alpha_s^0}{2\pi}G(\lambda)} \tag{B31}$$

where α_s^o is a coupling constant and $G(\lambda)$ is a function of variable λ which has different expressions given by the time-like momentum subtraction (the subtraction performed at time-like renormalization point) and the space-like momentum subtraction (the subtraction carried out at the space-like renormalization point). For the time-like momentum subtraction,

$$G(\lambda) = 11\ln\lambda - \frac{2}{3}N_f[2+\sqrt{3}\pi - \frac{2}{\lambda^2} + (\frac{2}{\lambda^2}+1)\frac{\sqrt{\lambda^2-4}}{\lambda}\ln\frac{1}{2}(\lambda+\sqrt{\lambda^2-4})] \tag{B32}$$

where N_f is the quark flavor number which will be taken to be three in this paper. While, for the space-like momentum subtraction,

$$\begin{array}{l} G(\lambda) = 11\ln\lambda - \frac{2}{3}N_f[\frac{2}{\lambda^2} - 2 - (\frac{2}{\lambda^2}-1)\frac{\sqrt{\lambda^2+4}}{\lambda}\ln\frac{1}{2}(\lambda+\sqrt{\lambda^2+4}) \\ +\sqrt{5}\ln\frac{1}{2}(1+\sqrt{5})] \end{array} \tag{B33}$$

in which λ is defined as $\lambda = \sqrt{q^2/\mu^2}$ with q being a momentum variable and μ the fixed scale parameter. It is noted that in writing the above effective coupling constant, the mass difference between different quarks is ignored for simplicity. In this paper, the effective coupling constants given in the space-like momentum subtraction and the time-like momentum subtraction are suitable for the t- channel OGEP and the s-channel OGEP, respectively.

The effective quark mass is represented as

$$m_R(\lambda) = m_R e^{-S(\lambda)} \tag{B34}$$

where m_R is the constant quark mass given at $\lambda = 1$ which will appropriately be chosen to be the constituent quark mass in the quark potential model, $S(\lambda)$ is a function which also has different expressions for the different subtractions. For the time-like momentum subtraction,

$$S(\lambda) = \frac{\alpha_R^0}{\pi}\frac{1-\lambda}{\lambda}\{2 + (\frac{2}{\lambda^2} - \frac{1+\lambda}{\lambda^2})\ln \mid 1-\lambda^2 \mid\}. \tag{B35}$$

In this paper, only the effective quark masses given in the time-like momentum subtraction is necessary to be considered.

VIII. REFERENCES

[1] Kumar K S and Nogami Y 1980 *Phys. Rev.* D **21** 1834.
[2] Veit E A, Jennings B K, Thomas A W and Barrett R C 1985 *Phys. Rev.* D **31** 1033.
[3] Jennings B K 1986 *Phys. Lett.* B **176** 299
[4] Batty C J 1990 *Nucl. Phys.* A **508** 89c.
[5] Schnick J and Landau R H 1987 *Phys. Rev. Lett.* **58** 1719; Fink Jr P J, He G, Landau R H, and Schnick J W 1990 *Phys. Rev.* C **41** 2720.
[6] Tanaka K and Suzuki A 1992 *Phys. Rev.* C **45** 2068.
[7] He G and Landau R H 1993 *Phys. Rev.* C **48** 3047.
[8] Arima M and Yazaki K 1990 *Nucl. Phys.* A **506** 553; Arima M, Matsui S and Shimizu K 1994 *Phys. Rev.* C **49** 2831.
[9] Siegel P B and Saghai B 1995 *Phys. Rev.* C **52** 392 and the references therein.
[10] Davies J D, Pyle G J, Squier G T A, Batty C J, Biagi S F, Hoath S D, Sharman P and Clough A S 1979 *Phys. Lett.* B **83** 55.
[11] Izycki M, Backenstoss G, Tauscher L, Blum P, Guigas R, Hassler N, Koch H, Poth H, Fransson K, Nilsson A, Pavlopoulos P and Zioutas K 1980 *Z. Phys.* A **297** 11.
[12] Bird P M, Clough A S and Parker K R 1983 *Nucl. Phys.* A **404** 482.
[13] Martin A D 1976 *Phys. Lett.* B **65** 346; 1981 *Nucl. Phys.* B **179** 33.
[14] Iwasaki M *et al* 1997 *Phys. Rev. Lett.* **78** 3067.
[15] Ito T M *et al* 1998 *Phys. Rev.* C **58** 2336.
[16] Kimura M *et al* 2004 *Phys. Rev.* C **62** 015206.
[17] Oset E, Ramos A and Bennhold C 2002 *Phys.Lett.* B **527** 99-105; 2002 *Erratum-ibid.* B **530** 260.
[18] Garcia-Recio C, Nieves J, Ruiz Arriola E and Vicente Vacas M J 2003 *Phys. Rev.* D **67** 076009.
[19] Choe S 1998 *Eur. Phys. J.* A **3** 65-73; 2000 *ibid.* A **7** 441-448.
[20] Magas V K, Oset E and Ramos A 2005 *Phys. Rev. Lett.* **95** 052301.
[21] Akaishi1 Y, Dote A and Yamazaki T 2005 *Phys. Lett.* **B 613** 140*;* Akaishi1 Y and Yamazaki T 2002 *Phys. Rev.* C **65** 044005.
[22] Magas V K, Oset E, Ramos A and Toki H 2006, arXiv preprint: nucl-th/0601013; Oset E and Toki H 2005 arXiv preprint: nucl-th/0509048.
[23] Agnello M *et al* (FINUDA Collaboration) 2005 *Phys. Rev. Lett.* **94** 212303; Suzuki T *et al (*KEK*)* 2004 *Phys.Lett.* B **597,** 263-269.
[24] Wang H J, Yang H and Su J C 2003 *Phys. Rev.* C **68** 055204.
[25] Griffin J J and Wheeler J A 1957 *Nucl. Phys.* **108**, 331.
[26] LEPS Collaboration, Nakano T *et al* 2003 *Phys. Rev. Lett.* **91** 012002.
[27] Kabana S 2005 arXiv: hep-ex/0503020 and reference therein.
[28] Karliner M, Lipkin H J 2004 *Phys. Lett.* B **597** 309-313 and the experimental references therein.
[29] Belle Collaboration (Abe K *et al*) 2006 *Phys.Lett.* B **632** 173-180.
[30] De Rújula A, Georgi H and Glashow S L 1975 *Phys. Rev.* D **12** 147.
[31] Su J C and Wu S S 1989 *Chinese Phys.* **8** 978; Su J C, Chen Z Q and Wu S S 1991 *Nucl. Phys.* **A 254** 615.
[32] Zhao G Q, Jing X G and Su J C 1998 *Phys. Rev.* **D 58** 117503.
[33] Chen J X, Cao Y H and Su J C 2001 *Phys. Rev.* **C 64** 065201.

[34] Braaten E and Fleming S 1995 *Phys. Rev. Lett.* **74** 3327.
[35] Cacciari M and Krämer M 1996 *Phys. Rev. Lett.* **76** 4128.
[36] Yuan F, Qiao C F and Chao K T 1997 *Phys. Rev.* **D 56** 1663 and references therein.
[37] Jaffe R and Wilczek F 2003 *Phys. Rev. Lett.* **91** 232003.
[38] Wei W, Huang P Z, Chen H X and Zhu S L 2005 *JHEP* **0507** 015 and the reference therein.
[39] Hyodo T and Hosaka A 2005 *Phys.Rev.* D **71** 054017 and the references therein.
[40] J. C. Su, L. Y. Shan, Y. H. Cao, Commun. Theor. Phys. 36, 665 (2001).
[41] Hyslop J S, Arndt R A, Roper L D and Workman R L 1992 *Phys.Rev.* **D 46** 961.
[42] Hashimoto K 1984 *Phys. Rev.* **C 29** 1377.

IX. FIGURE CAPTIONS

Fig.1: The theoretical $\overline{K}N$ S-wave phase shifts in the $I = 0$ and 1 channels.

Fig.2: The theoretical $\overline{K}N$ P_{01}-wave and P_{13}-wave phase shifts.

Fig.3: The theoretical KN P_{01} phase shift. The experimental phase shift [41, 42] are shown by black squares with error bars.

Fig.4: The theoretical KN D_{03} phase shift. The experimental phase shift [41, 42] are shown by black squares with error bars.

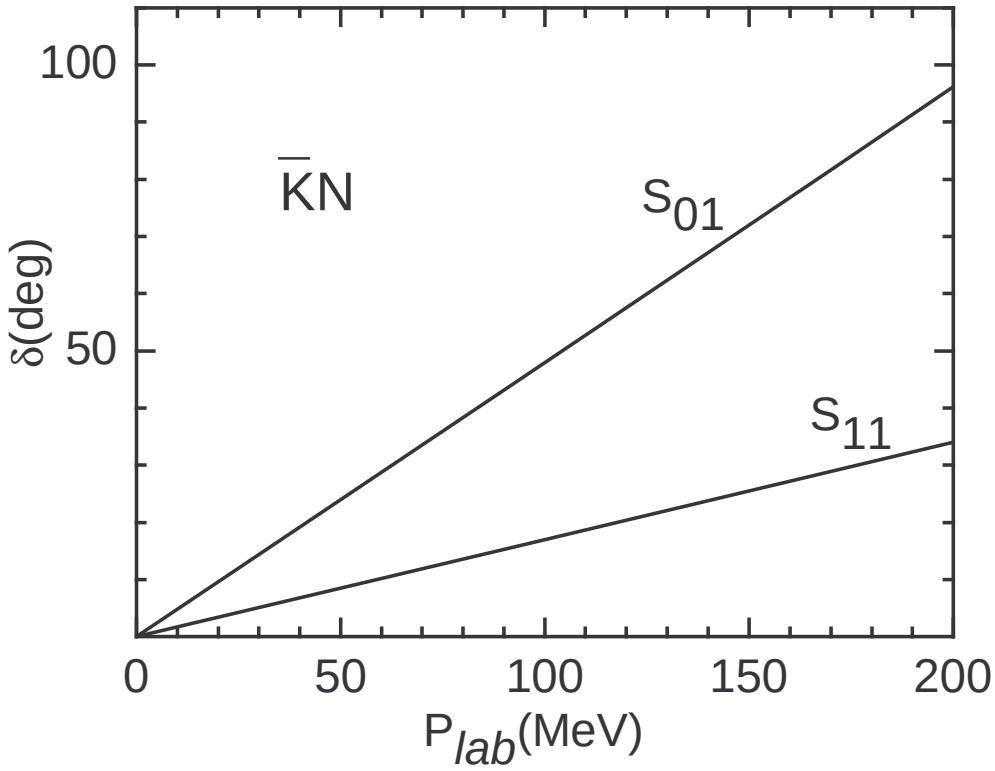
100
50
δ(deg)
$\bar{K}N$
S_{01}
S_{11}
0
50
100
150
200
P_{lab}(MeV)

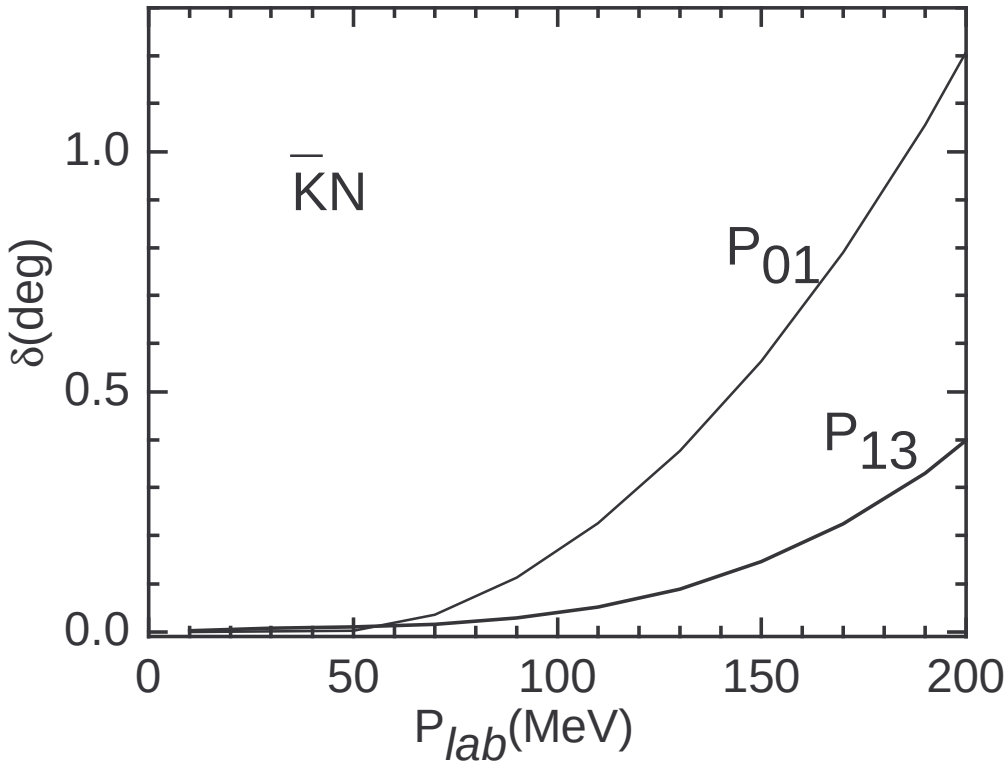
1.0
0.5
0.0
δ(deg)
$\bar{K}N$
P_{01}
P_{13}
0
50
100
150
200
P_{lab}(MeV)

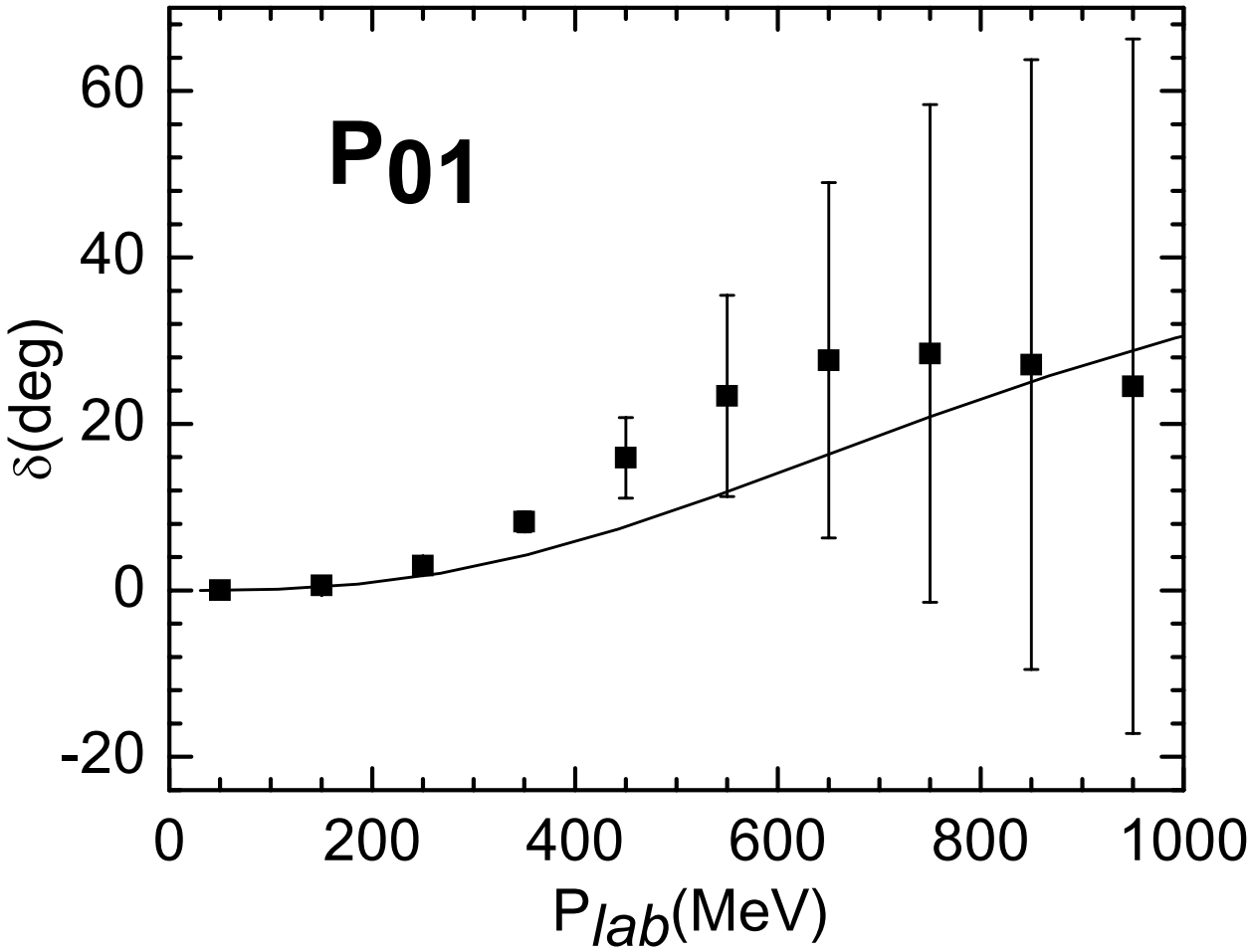
P01
δ(deg)
60
40
20
0
-20
0
200
400
600
800
1000
P lab (MeV)

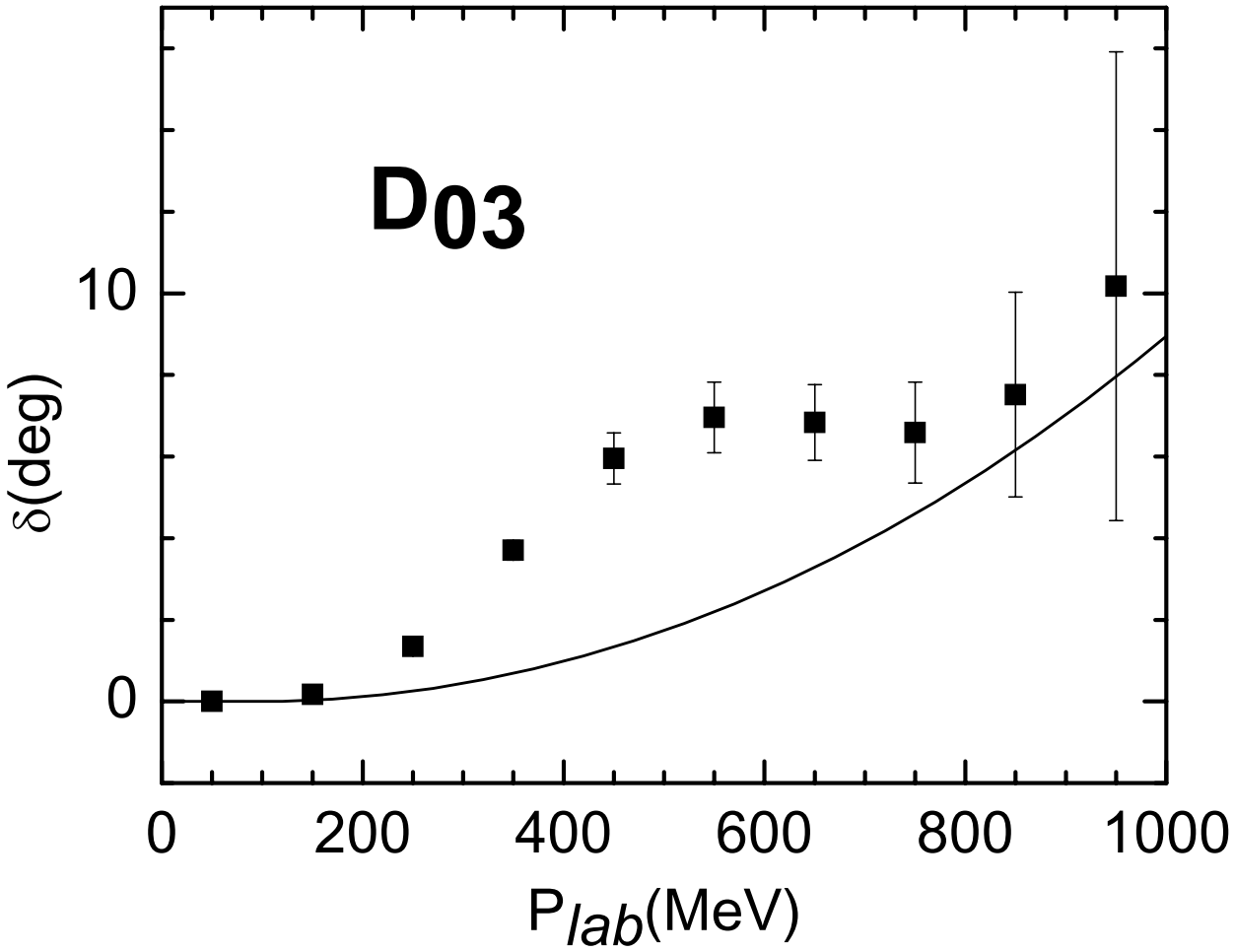
D03
10
0
δ(deg)
0
200
400
600
800
1000
P lab (MeV)